DECENTRALIZED CONTROL OF DC MICROGRIDS WITH ENERGY STORAGE SYSTEMS

BY

MD. JUEL RANA

A Thesis Presented to the
DEANSHIP OF GRADUATE STUDIES

KING FAHD UNIVERSITY OF PETROLEUM & MINERALS

DHAHRAN, SAUDI ARABIA

In Partial Fulfillment of the
Requirements for the Degree of

MASTER OF SCIENCE

In

ELECTRICAL ENGINEERING

JANUARY 2017

KING FAHD UNIVERSITY OF PETROLEUM & MINERALS

DHAHRAN- 31261, SAUDI ARABIA

DEANSHIP OF GRADUATE STUDIES

This thesis, written by **MD. JUEL RANA** under the direction his thesis advisor and approved by his thesis committee, has been presented and accepted by the Dean of Graduate Studies, in partial fulfillment of the requirements for the degree of **MASTER OF SCIENCE IN ELECTRICAL ENGINEERING**.

Dr. Mohammad Ali Abido
(Advisor)

Dr. Ali Ahmed Al-Shaikhi
Department Chairman

Dr. Ibrahim Mohamed ElAmin
(Member)

Dr. Salam A. Zummo
Dean of Graduate Studies

Dr. Ibrahim Omar Habiballah
(Member)

18/1/17

Date

[*Dedicated To my Father*]

ACKNOWLEDGMENTS

At first, I am grateful to the almighty Allah for giving me ability to accomplish this thesis. Without His mercy and blessing nothing is possible.

I would like take the chance to express my gratitude toward Dr. Mohammad Ali Abido for his sagacious supervision. He taught me how to overcome the hurdles of research works with steadfastness and perseverance. His problem specific directions with vast research expertise and continuous motivation make it possible to finish the work successfully.

I am also thankful to my course teachers Dr. Ibrahim Mohamed ElAmin and Dr. Ibrahim Omar Habiballah. The technical knowledge gained from their educated teaching helped me a lot throughout my works.

I would like to thank all the members of power research group for their support during this work. It is worthwhile to mention PhD researchers Md Shafiullah, Shafiul Alam and Mohamed Mamdouh for their valuable suggestions time to time.

Last but not least, I am immensely indebted to my parents, sisters and brothers for their endless love and psychological support. I am thankful to my elder brother Dr. Abul Hossain Mondal for his encouragement for my higher study.

TABLE OF CONTENTS

LIST OF TABLES

LIST OF FIGURES

LIST OF ABBREVIATIONS

BESS	:	Battery Energy Storage System
CC-CV	:	Constant Current-Constant Voltage
DG	:	Distributed Generation
ESS	:	Energy Storage System
EDLC	:	Electric Double Layer Capacitor
MG	:	Microgrid
MPC	:	Model Predictive Control
MPP	:	Maximum Power Point
MPPT	:	Maximum Power Point Tracking
PI	:	Proportional Integral
PV	:	Photovoltaic
RES	:	Renewable Energy Source
RTDS	:	Real Time Digital Simulator
RTHIL	:	Real Time Hardware in the Loop
SMES	:	Superconducting Magnetic Energy Storage
SoC	:	State of Charge

VSC : Voltage Source Converter

LIST OF SYMBOLS

I_{PV}	:	PV panel output current
V_{PV}	:	PV panel output voltage
a	:	Diode ideality factor
I_D	:	Diode current
N_S	:	Number of cells in the PV panel
k	:	Boltzmann's constant
q	:	Electronic charge
D	:	Duty cycle for DC-DC converter
C_{DC}	:	DC link capacitor
I_{DC}	:	DC link current
V_{DC}	:	DC link voltage
f	:	Switching frequency
V_{Batt}	:	Battery terminal voltage
I_{Batt}	:	Battery output current
V_{SC}	:	Supercapacitor terminal voltage
I_{SC}	:	Supercapacitor output current

V_{OC}	:	Battery open circuit voltage
V_{ST}	:	Voltage across energy storage devices
L_s	:	Inductance of AC grid interface reactor
R_s	:	Resistance of AC grid interface reactor
SoC	:	State of Charge
$\vec{v}_s$	:	Voltage vector of three phase AC source
$\vec{i}_s$	:	Current vector of three phase AC source
$\vec{v}$	:	Voltage vector of AC-DC converter
$\vec{S}_w$	:	Switching state vector of AC-DC converter
T_s	:	Sampling time
J	:	Cost function for optimization
P^{ref}	:	Reference real power
Q^{ref}	:	Reference reactive power
i_d	:	Direct axis component of three phase current
i_q	:	Quadrature axis component of three phase current
P_{load}	:	Load power
P_{PV}	:	PV power

P_{grid}	:	AC Grid power
$P_{storage}$	:	Energy storage power
K_P	:	Proportional gain
K_I	:	Integral gain

ABSTRACT

Full Name : [Md. Juel Rana]

Thesis Title : [Decentralized Control of DC Microgrids with Energy Storage Systems]

Major Field : [Electrical Engineering]

Date of Degree : [January 2017]

[The concept of DC microgrid is gaining significant interest due to its several advantages over AC microgrid. DC microgrid facilitates high penetration of renewable energy sources to the grid and contributes to the global reduction of carbon footprint.

The voltage regulation of DC microgrid is a challenging task in order to prevent circulating current among different distributed energy sources connected in parallel. Another crucial issue is to manage active power among the distributed sources, loads and connected utility grid. Energy storage systems help to combat these challenges. In this work, a small scale DC microgrid is considered which is comprised of photovoltaic energy source, local loads and hybrid energy storage system. A decentralized control strategy based on DC bus voltage regulation is proposed for energy management in the system. Model predictive controller is proposed to regulate the power exchange between microgrid and utility grid. Frequency based power sharing approach of energy storage devices is proposed for voltage regulation in the microgrid. The system model for the microgrid system as well as its control strategies are developed using RSCAD software and simulated using real time digital simulator (RTDS) for various operating conditions. Real time hardware in the loop experiments are performed to validate the effectiveness of proposed control strategies.]

ملخص الرسالة

الاسم الكامل: محمد جويل رنا

عنوان الرسالة: مراقبة اللامركزية من DC Microgrids مع نظم تخزين الطاقة

التخصص: : الهندسة الكهربائية

تاريخ الدرجة العلمية: يناير 2017

لقد اكتسب مفهوم ال DC microgrid اهتماما كبيرا بسبب العديد من المزايا التي فاقت تلك الموجودة في AC microgrid. إن مفهوم ال DC microgrid يسهل عملية اختراق عالية لمصادر الطاقة المتجددة إلى الشبكة، ويسهم في تخفيض انبعاثات الكربون.

ويجري أيضا تنفيذ كهربة نظام النقل للحد من انبعاثات الكربون. تنظيم جهد ال DC microgrid هو مهمة صعبة من أجل منع تداولها بين مصادر الطاقة الموزعة المختلفة والمتصلة على التوازي. هناك قضية حاسمة أخرى وهي إدارة الطاقة النشطة بين توزيع المصادر، والأحمال وشبكة المرافق المتصلة.إن نظم تخزين الطاقة تساعد على مكافحة هذه التحديات.في هذا العمل، تم استخدام مفهوم ال DC microgrid على نطاق ضيق يتألف من مصدر الطاقة الضوئية، والأحمال المحلية ونظام هجين تخزين الطاقة. تم اقتراح استراتيجية مكافحة اللامركزية على أساس ال DC microgrid لتنظيم حافلة الجهد لإدارة الطاقة في النظام. ويقترح نموذج التحكم التنبؤي طريقة لتنظيم تبادل الطقاة بين microgrid وشبكة المرافق. كما يقترح النهج القائم على تقاسم طاقة التردد من أجهزة تخزين الطاقة لتنظيم الجهد في microgrid.كذلك, تم تطوير نموذج لنظام microgridو استراتيجيات التحكم الخاصة به باستخدام برنامج RSCAD ومحاكاة في محاكاة رقمية في الوقت الحقيقي لظروف التشغيل المختلفة. تم تنفيذ الأجهزة في الوقت الحقيقي في التجارب للتحقق من فعالية استراتيجيات الرقابة المقترحة.

CHAPTER 1

INTRODUCTION

1.1 Motivation

The power system networks worldwide are dominated by AC systems. The revolutionary advancement of semiconductor technology and the power electronic converters creating increasing interest on implementation of the DC power systems. The rising attention for DC system lies in the inherent advantages of the DC system over the AC one. Many domestic loads such as computers, microwave oven, lighting consumes DC powers and conversion of AC to DC causes significant energy loss which is about 10-25% [1]. In industrial applications, like DC electric arc furnaces consume less energy than AC furnaces [2]. The concerted emphasis on the higher penetration of environment friendly renewable energy sources (RES) into the power system is another catalyst for development of DC systems. The DC based RES such as photovoltaic (PV) and fuel cells can directly be integrated in the network which avoids the conversion stages and thus increase the energy efficiency of the system [3]. The use of energy storage (ES) technology which increases the reliability of power supply is more facilitated by the DC than AC systems.

Microgrid (MG) is defined as the controllable local energy network that includes distributed generations (DGs), loads and storage systems. Due to simpler structure and higher energy efficiency of the DC systems, the concept of DC microgrid is gaining popularity [3]. The

technology of AC MG has already been established whereas DC MG technology still requires further research to resolve the challenges of stable and reliable implementation.

The operation of DC microgrid is simpler than the AC grid due to the absence of phase, frequency and reactive power. It is required to balance active power to maintain the DC bus voltage in a DC microgrid [4]. DC microgrid also does not increase the short circuit capacity of the main grid at the point of common connection (PCC) due to the interconnecting AC-DC converter and this converter also prevents the power quality problems on the DC side [5].

1.2 Challenges

Although, DC microgrids have several advantages over its AC counterpart, it needs further improvement in the area of control technology, developing standards and protection system.

The DC microgrid contains distributed energy sources, loads and energy storage systems which are connected in parallel to a common DC bus. The main challenges of DC microgrid include regulating the DC bus voltage and effective power sharing among the distributed sources [6]. Deviation in the common DC bus voltage will create circulating current among energy sources. The power sharing among distributed generators need to be based on their rating or cost otherwise it will make the system uneconomical and unbalanced.

Energy storage system increases reliability of the microgrid; However, single energy storage technology is not sufficient for that purpose. To handle intermittency of renewable generation, energy storage technology with high energy density such as battery storage is demanded. But, in order to take care of the high frequency load fluctuation or power transients the storage technology having faster response and large power density is demanded. The composite of high power density and high energy density storage technology can solve this problem. Energy

management of the composite storage system requires improved control strategy to ensure reliability of the microgrid.

1.3 Objectives of the Thesis

This thesis work intends to achieve the following objectives:

- To develop a model of a low voltage DC microgrid with photovoltaic (PV) and hybrid energy storage system having supercapacitor and battery
- To design a new decentralized control strategy for effective power management among the different modules of DC microgrid and utility grid
- To perform real time simulation using RTDS to investigate the performance of the proposed control strategy by considering different modes of operation of the microgrid and system perturbation.
- To perform real time hardware in the loop experimental tests using RTDS and DS1103 controller board to test the effectiveness of the designed controllers.

1.4 Contributions of the Thesis

Major contributions of the thesis are listed below.

- Development of a low voltage DC microgrid model with PV and hybrid energy storage comprising of battery and supercapacitor
- Design of effective control strategy for power management during islanded and grid connected mode of microgrid
- Development of system model and control strategy using RSCAD software and RTDS based real time simulation works to verify the controller performance.

- Real time hardware in the loop experimental test of the simulated system using RTDS and dSPACE platform

1.5 Organization of the Thesis

The literature review related to the thesis work is presented in Chapter 2. The literature review presents the different control strategies for DC microgrid. The pros and cons of the control techniques are addressed.

Chapter 3 includes system model of a photovoltaic based DC microgrid. Proposed control strategies for energy management in the microgrid are presented. Chapter 4 presents the RTDS based simulation results as well as real time hardware in the loop experimental results for DC microgrid. Chapter 5 concludes the thesis and proposes some future works.

CHAPTER 2

LITERATURE REVIEW

2.1 DC Microgrid

In the recent years, increasing attention to the DC microgrid has been observed due to its potential advantages over the AC counterpart such as [6]

- Control in DC is easier as there is no reactive power and frequency
- Less number of power conversion stage required thus reducing overall cost and increasing efficiency
- DC system is not exposed to high fault current as it is limited by the power electronic converter

In DC microgrid power sources (renewable or non- renewable), loads, energy storage system (ESS), and converter for grid interfacing all are connected in parallel with the common DC bus. The main challenges faced by the DC system in paralleling the power sources are: (1) controlling the DC bus voltage which is essential for system stability and requires proper design of power converter (2) effective load sharing of the sources depending on their rating or cost. In this case source output impedance plays a vital role [7].

In order to regulate the DC bus voltage and load sharing among the sources a stable control system need to be designed.

In a general manner, the microgrid control system can be categorized as decentralized, centralized, and hybrid. The dependence of the centralized controller on the communication

channel may jeopardize the system reliability in case of any communication failure [4]. Decentralized control does not require communication channel but exhibits poor voltage regulation. On the other hand, the hybrid control utilizes the good features of both centralized and decentralized control. The aforementioned control strategies may be included under hierarchical control. The next sections present the hierarchical control and intelligent control in DC microgrids.

2.2 Hierarchical Control

In hierarchical control, there are three control levels of hierarchy: primary, secondary and tertiary. This control architecture increases the system flexibility enabling integration of more distributed power sources. This control strategy also works for different operating modes of the microgrid: grid connected mode, islanding mode and load shedding or generation curtailment mode [8].

The primary control level regulates the load sharing among distributed power sources based on the droop characteristics of the interfacing power electronic converters. The secondary control deals with voltage fluctuation control and also responsible for restoration and synchronization of DC grid with other grids. The tertiary control handles the energy management [6].

2.3 Primary Control

In order to regulate the output voltage and power sharing among distributed generations two methods are used. These are (i) passive control method (droop concept) and (ii) active load sharing method.

In DC microgrid applications, droop control is a widely used method for effective load sharing among the parallel power sources connected to the common bus. In AC microgrid, the droop concept is the variation of active and reactive power of synchronously rotating AC generators

with respect to frequency and generator terminal voltage respectively [9]. But in case of DC microgrid the droop concept means the variation of active power with respect to DC voltage. The load sharing can be maintained without the need of communication system. In DC microgrid, the droop characteristics of power electronic converters can be expressed as a linear function of voltage and current or power and voltage [6].

However, the conventional droop control technique suffers from some drawbacks like tradeoff between current sharing and voltage regulation as well as creating circulating current among DGs connected through power converters.

For V-I droop characteristics, voltage regulation is good for small droop but current sharing is poor and opposite occurs for large droop. On the other hand, the P-V droop characteristics exhibits opposite behavior that of V-I droop [10] [11].

Therefore, a tradeoff between load sharing and voltage regulation needs to be made while applying the droop concept. In the literatures it is found that researchers proposed a control strategy to overcome this drawback. For proper load sharing among the interfacing power converters to the common bus the droop control method or its variants have been widely used [11]. In [11] fuzzy and gain scheduling based control technique is applied to obtain better voltage regulation, load sharing as well as energy balance of the storage devices. The droop concept is applied to maintain current sharing among different sources connected in a DC nanogrid as presented in [12].

The problem of circulating current in droop method can be overcome using two methods: (i) putting identical series resistor with all DG output (ii) virtual output resistance method [6].

For DC microgrid application second method is more suitable due to its lower loss than first one and this method is analogous to the virtual or fictitious impedance method of AC microgrid. In droop control of DC microgrid, fraction of the converter output current is subtracted which is proportional to the virtual resistance (VR) at no load [13]. In this control scheme the converter output current varies inversely with its virtual resistance. The voltage deviation originated from droop characteristics depends on load current and the value of virtual resistance. This voltage deviation is an inherent limitation of droop concept. To keep this deviation within tolerable range, virtual resistance is limited by the equation (2.1) given below.

$$R_{di} \leq \frac{\Delta V_{dci\ max}}{I_{dcfli}} \tag{2.1}$$

Where, I_{dcfli} and $\Delta V_{dci\ max}$ are the full load output current and maximum acceptable voltage deviation for the ith converter [14].

A variant of droop control named voltage-based power–voltage control method (VbPV) is presented in [15]. This method provides almost rated voltage profile that is essential for critical loads. It also reduces voltage drops in DC microgrid with long lines and suppresses circulating currents.

The active load sharing methods are categorized into four types: (i) centralized control (ii) master-slave control (iii) circular chain control and (iv) average load sharing method. These control methods provides better load sharing and voltage regulation than the passive load sharing method [16]. However, these methods requires communication channel among different modules which makes system complex and reduces reliability in case of communication failure.

2.4 Secondary and Tertiary Control

For stable operation of DC microgrid it is essential to minimize voltage fluctuation as well as keeping energy balance at different operating modes. The secondary control corrects the voltage deviation introduced in the primary control. Tertiary control deals with the energy management strategies for grid connected, islanded, and transition periods. Depending on the type of secondary control the energy management strategies can be categorized as centralized, decentralized, and hybrid.

2.4.1 Centralized Control

The centralized controller takes information from different local parts of the system and sends necessary signals for corrective measure to rectify voltage deviation or energy management problems. This strategy gives optimal performance but requires real form of communication system which makes the system complex and reduces system reliability in case of communication failure.

A two layer battery management strategy in an autonomous DC microgrid is presented in[13]. The primary control layer is based on adaptive voltage droop method which regulates DC bus voltage and balances the state of charge (SoC) of the batteries. The supervisory control layer uses low bandwidth communication system to calculate virtual resistance (VR) for transition among different operating modes of the system. However, the incorporation of communication system may cause single line of failure which hampers reliability.

2.4.2 Decentralized Control

In the decentralized control decisions for any corrective actions are made at the local controllers. Decentralized control can be (a) with communication and (b) without

communication. In the decentralized control with communication system information is shared between different modules of the microgrid but decisions are made at local controllers.

(a) With Communication

The droop control method with low bandwidth communication (LBC) system has been used for restoration of DC bus voltage and current sharing among converters [17]. Here, local current and voltage controllers were used for each converter for proper current sharing and voltage regulations. The LBC was used to exchange voltage and current information among converters. However, the system exhibits oscillatory behavior with large communication delay as large as 1 second.

The operation of a hybrid AC-DC microgrid is presented in [18]. The authors designed hierarchical control on the DC side and employed droop control in primary level of control for proper DC output load current sharing. The voltage deviation originated from droop control was tackled by LBC based secondary control. The effect of communication delay both in secondary and tertiary control level was simulated by Eigen value analysis to validate stability margin.

In [10] authors proposed decentralized droop based control strategy in order to achieve effective load sharing and better voltage regulation in low voltage DC microgrid. They used low bandwidth communication (LBC) to overcome the shortcomings of conventional droop control.

In [19] the authors proposed a coordination strategy among different units of DC microgrid using power line signaling (PLS). Here, power line is used as a communication channel to exchange information among different units. The units injects sinusoidal signal with specific frequency into common DC bus from the primary control loop to share information with each other and upon reading the signal from primary controller the units local controller respond

accordingly by changing their mode of operation. Any deviation in the common bus voltage due to local controller actions is tackled by secondary control. However, this control strategy suffers from slow communication speed through power line signaling.

(b) Without Communication

Communication free decentralized control has been presented in [20] to acquire balanced load sharing among energy storage units. In this work, state of charge (SoC) based adaptive droop control is used where the storage units discharge power based on their droop setting that is inversely proportional to their SoC. The storage with large SoC discharge faster and vice versa which gradually leads to equal SoC of the units. The authors extended their work in [21] by presenting double quadrant SoC based droop control method which considers both charging and discharging mode of operation.

A decentralized energy management strategy of a low voltage stand-alone DC microgrid is presented in [22]. The control technique is based on bus signaling method. A secondary control is used to restore voltage deviation caused by primary control. To ensure reliable service of a DC microgrid having critical load a control strategy based on DC bus signaling method is also presented in [23].

In [24] decentralized control strategy is proposed for autonomous operation of a hybrid microgrid. The control method regulates local power sharing in individual network (AC/DC), global power sharing between AC and DC network and distributed power sharing among distributed storages. The droop based local control modules can operate independently without the need of communication link and thus increase reliability.

2.4.3 Hybrid Control

In order to achieve better result, the hybrid control structure accommodates the advantages of aforementioned techniques for better performance. A hybrid control strategy is proposed for optimal operation of a stand-alone DC microgrid in [25]. As part of the central energy management the authors used communication system to observe bus voltages, power flow and converter status. In case of any failure of communication link, DC bus signaling technique is proposed as back up control strategy.

2.5 Intelligent Control

For extremely complex and uncertain system the intelligent control techniques performs better than classical ones. In the literatures use of intelligent control techniques has been reported for DC microgrid applications.

In [11] the authors used fuzzy logic control and gain scheduling technique for proper controlling of electric double layer capacitor storage system. Here gain scheduling is used for voltage control and fuzzy logic is used for balancing the stored energy. Application of Fuzzy logic control for DC voltage control was also reported in [26].

2.6 Energy Storage System (ESS)

In microgrid applications, normally the generation capacity is very close to the load power demand. Energy storage system is essential for stable operation of DC microgrid in case of any discrepancy between the total generation and total load of the system. One of the goal of microgrid application is to facilitate the integration of the renewable energy sources. But the intermittent power generation from the renewable sources may cause the instability in the system especially in islanded mode of operation of microgrid. In microgrid, energy storage system serves as spinning reserve in the conventional power system to maintain the power

balance [27]. Quick response ESS can effectively minimize electromechanical oscillations in the power system by sharing sudden change in power requirement [28]. Therefore, in DC microgrid energy storage system is required to maintain stability, increase penetration of renewables and also to improve the power quality.

In the literatures, various energy storage system have been reported for use in the DC microgrid application such as batteries [29], electric double layer capacitors [30], flywheel energy storage (FES) [31] and superconducting magnetic energy storage system (SMES) [32].

2.6.1 Battery Energy Storage System (BESS)

Battery stores energy electrochemically and it is one of the most cost effective energy storage technologies. Battery energy storage system is formed by series and parallel combination of low voltage/power battery module in order to get the desired electrical characteristics. In microgrid applications, lead-acid batteries are widely used to form BESSs for their high energy density. Lead-acid batteries can be valve regulated and flooded type. The valve regulated battery is more reliable due to its less maintenance requirement [33][34][35].

In [29] the authors presented the control of BESS for both grid connected and islanded mode of a PV based DC microgrid. They validated the simulation results with experimental test and used lead-acid batteries for that purpose. The results demonstrated the efficacy of proposed control scheme in controlling DC voltage and maintain stable microgrid operation.

The operation and control system of DC microgrid consisting of wind generation, battery energy storage system, variable loads and AC grid has been presented in [36]. The authors proposed control system to maintain DC voltage of microgrid for three operating modes: normal grid connected mode, grid fault mode and islanded mode.

A power flow control strategy of an islanded hybrid AC-DC microgrid consisting of PV system, battery energy storage and pulse load was presented in [37]. The proposed coordinated control strategy was demonstrated with simulation results.

2.6.2 Electric Double Layer Capacitors (EDLC)

Electric double layer capacitor (EDLC) consists of two electrodes inserted into an electrolyte and separated by dielectric material. The two electrodes of the capacitor hold micropores and provide surfaces for the charges to build up. Electrostatic energy is stored in the dielectric material. The EDLCs are also known as ultra-capacitors or supercapacitors[38].

The EDLCs have high power density compared to battery energy storage. They exhibits faster response, need low maintenance and have longer life cycles due to absence of chemical reaction. However, due to their limited energy storage capability they are suitable for short term storage [39][38].

In [40] supercapacitor is used as main energy storage system for a low voltage bipolar residential DC microgrid. The supercapacitor storage system is used for regulating the DC bus voltage during islanding mode and for voltage clamping during grid connected mode if DC distribution voltage exceeds the maximum limit.

Energy management in a droop controlled DC microgrid using supercapacitor is proposed in [41]. The supercapacitor energy storage system is used to compensate the surge current caused by the step change in the load. Virtual impedance method is used to decouple the power transfer between supercapacitor and other distributed generations in the microgrid.

The control system of ultra-capacitor based energy storage system employed in DC microgrid is proposed in [30]. The authors proposed a Proportional Integral Resonant (PIR) controller to

regulate the DC bus voltage by controlling the charging and discharging of ultra-capacitor under all operating condition of microgrid.

2.6.3 Flywheel

Flywheel storage system works in the way that it stores energy in the spinning mass when the mass is accelerated by an electrical drive. The stored energy can be retrieved by making the machine to work in the regenerative breaking to slow down the mass. Flywheel provides fast response, high storage capacity and high efficiency. But, flywheel storage system can store energy for short duration only [38].

In [31] the authors used a squirrel cage induction motor as flywheel in DC microgrid. The flywheel controls the DC voltage by absorbing or supplying load generation imbalance.

Flywheel energy storage system to use with DC microgrid is also reported in [42]. The authors used active disturbance rejection control to improve the performance of the flywheel energy storage system.

2.6.4 Superconducting Magnetic Energy Storage (SMES)

In SMES energy is stored in the magnetic field when current passes through an inductor. The term superconducting originates from the fact that the inductor is fabricated from a superconducting material which shows zero resistance at low temperature. The stored energy in the inductor owing to the application of positive voltage is transferred back to the electrical system with the application of reverse voltage across the inductor. It provides high efficiency and faster response, but this storage technology is costly [38].

The SMES is used for enhancing low voltage ride through capability and minimizing power fluctuation in a DC microgrid with doubly fed induction generator (DFIG) based wind turbine [32].

In [43] SMES is used for improving transient performance of the microgrid. For improving fault ride through capability SMES is used in conjunction with fault current limiter which enables smooth transition between grid connected and islanded modes of microgrid.

2.6.5 Hybrid Energy Storage

A single type of energy storage system is not sufficient for effective energy management in different operating modes of renewables based microgrid. To compensate for the system oscillation caused by uncertainty of renewable power generation energy storage system of higher energy density is required. On the other hand, the high frequency oscillation caused by quick load variation or fault in the system needs energy storage system having higher power density and faster response. To achieve both requirements a hybrid energy storage system need to be adopted.

A composite energy storage system comprised of battery energy storage (high energy density) and ultra-capacitor (high power density) was presented in [44]. Dual active bridge DC-DC converter was used as the interface between storage system and DC grid. Active energy management strategy between battery and ultra-capacitor was demonstrated with case studies and results were validated with experimental setup.

The energy management of a decentralized generation system including wind generation, PV and energy storage system is presented in [45]. The authors proposed frequency approach to share the fluctuating power of wind/load between ultra-capacitor and battery storage. They also used polynomial controller to estimate the energy storage capacity.

2.7 Summary of Literature Review

The literature review conducted for this work presents the different control strategies for DC microgrid applications. The control strategies include hierarchical control and intelligent

control. The hierarchical control includes all the control levels for the microgrid operation such as primary, secondary and tertiary control. In general, these control level has also been categorized as centralized, decentralized and hybrid control. The use of centralized controller may disrupt the system operation in case of any failure in the communication link required for this. Furthermore, the use of communication system increases the complexity and overall cost of the system.

The communication free decentralized control schemes have widely been reported in the literatures due to their less complexity and higher reliability of operation. The autonomous decentralized control strategies also increase the flexibility in the system facilitating the integration of distributed generation in the DC microgrid.

The high integration of intermittent renewable energy sources to the microgrid poses system instability by creating load generation imbalance. To take care of this incident the use of energy storage system has been reported in the literatures. Among all other storage system BESS and EDLC have been widely used for DC microgrid applications. Having high power density BESS can regulate the DC bus voltage by supplying or absorbing power imbalance in the grid. On the other hand, EDLC has low power density but faster response than BESS. This is why EDLC can provide fast compensation for voltage fluctuation during transients. Therefore, to handle low frequency as well as high frequency disturbances in the system a hybrid energy storage system is essential.

In order to overcome the complexity and lower reliability associated with the centralized control strategy, this thesis aims to employ decentralized control technique for operation of the DC microgrid. Decentralized control based on DC bus signaling is proposed which uses bus voltage

as the information carrier to maintain the power balance in the microgrid. The proposed control strategy not only simplifies the control approach but also improves the reliability of the system.

CHAPTER 3

SYSTEM MODEL AND CONTROL DESIGN

3.1 System Model

A PV based small scale DC microgrid has been considered in this work as shown in Figure 3.1. The DC microgrid is connected with the utility grid through bidirectional voltage source converter and contains PV as the renewable energy source. Different types of local loads (resistive and power electronic interfaced) have been considered lumped. PV panel, energy storage system (ESS) and voltage source converter (VSC) are connected to the common DC bus.

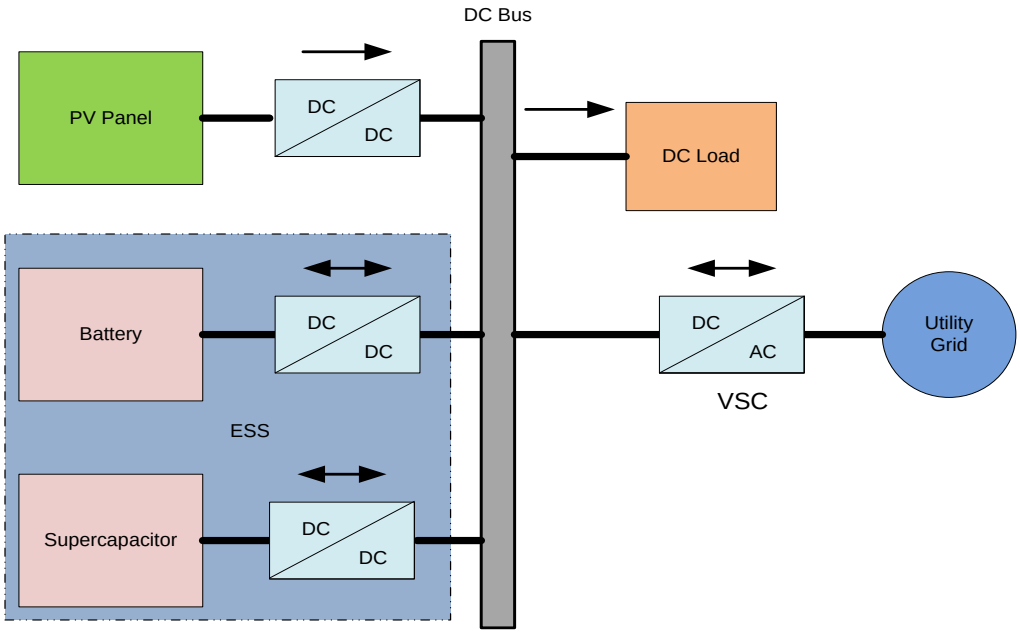

Figure 3.1: Schematic of DC microgrid

The purpose of the energy storage unit is to smooth out the power fluctuation caused by variation in the renewable power generation, load and utility power demand. Single kind of energy storage system is not capable of handling the power fluctuation as well as the transients caused by these power variations. As suggested by theory of Ragone plot [46] hybrid storage system comprised of battery and supercapacitor has been considered to overcome this problem. Hybrid system has the characteristics of both high power and high energy density as well as extends the battery lifetime.

3.2 PV Modeling

The PV array is connected to the DC microgrid as a distributed generator (DG) unit through buck converter. The equivalent circuit model of the PV array [47] is shown in Figure 3.2.The equivalent circuit consists of a light dependent current source, p-n junction diode, series and shunt resistance. The currents of the circuit are represented by equations (3.1)-(3.4) [48].

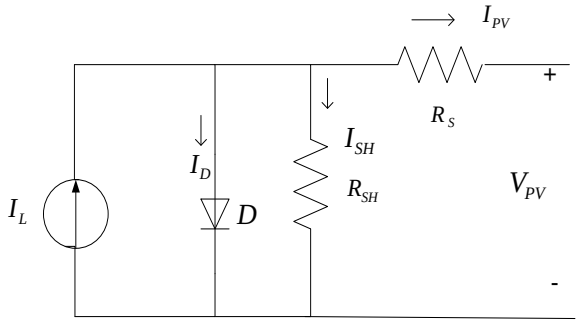

Figure 3.2: PV array model

$$I_{PV} = I_L - I_D - I_{SH} \tag{3.1}$$

$$I_D = I_0\{\exp[\frac{V_{PV} + I_{PV}R_S}{a}] - 1\} \tag{3.2}$$

$$I_{SH} = \frac{V_{PV} + I_{PV} R_S}{R_{SH}} \tag{3.3}$$

$$I_D = I_L - I_0 \{\exp[\frac{V_{PV} + I_{PV} R_S}{a}] - 1\} - \frac{V_{PV} + I_{PV} R_S}{R_{SH}} \tag{3.4}$$

Where,

I_D	:	diode current,
I_{SH}	:	current through shunt resistor,
V_{PV} and I_{PV}	:	PV panel voltage and current respectively
I_L	:	light generated current,
I_0	:	diode saturation current,
R_S and R_{SH}	:	series and parallel resistance respectively
a	:	diode modified ideality factor given by equation

$$a = \frac{N_s n k T}{q} \tag{3.5}$$

Where,

N_S	:	number of cells in the PV panel,
n	:	ideality factor (it has a value between 1 to 2 for real diode)
k	:	Boltzmann's constant,
T	:	cell temperature and
q	:	electronic charge

3.3 Modeling of Buck Converter

The buck converter has been used as an interface between PV and DC link. The main task of buck converter is to regulate the unregulated PV output voltage based on the reference voltage generated from maximum power point tracking (MPPT) controller. The reference voltage from

MPPT is for the maximum power generation from PV. The circuit diagram of the buck converter is shown in Figure 3.3.

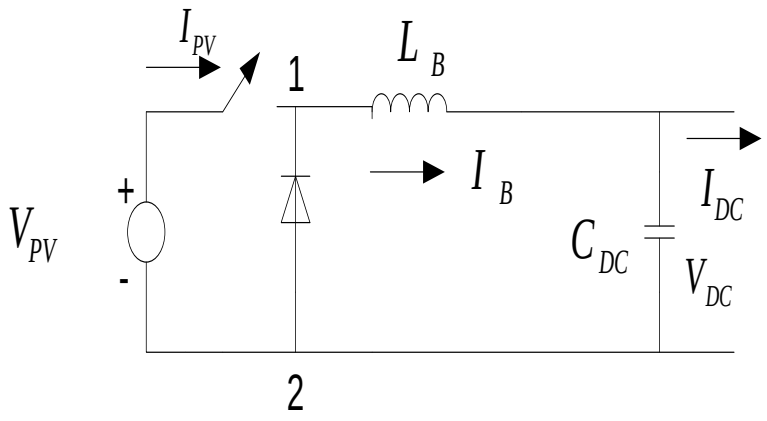

Figure 3.3: Buck converter

The buck converter has two modes of operation. In mode 1, the switch is turned on, which increases the inductor current linearly. In mode 2, the switch is turned off, the diode get forward biased and the energy stored in inductor in mode 1 cause the current flow. In this case, inductor current decreases linearly. The differential equation representing the DC buck converter model is obtained as follows [49]:

In mode 1, applying KVL we can write

$$V_{PV} - L_B \frac{dI_B}{dt} - V_{DC} = 0 \tag{3.6}$$

$$\frac{dI_B}{dt} = \frac{V_{PV} - V_{DC}}{L_B} \tag{3.7}$$

The DC link voltage in terms of PV output voltage is expressed as following equation.

$$V_{DC} = DV_{PV} \tag{3.8}$$

$$I_B = DI_{PV} \tag{3.9}$$

Where,

L_B : buck converter inductor

I_B : buck converter inductor current

D : duty of the buck converter

V_{DC} : DC link voltage

C_{DC} : DC link capacitor

I_{DC} : DC link current

The value of the inductor can be calculated from the following equation.

$$L_B = (V_{PV} - V_{DC})\frac{1}{f} * \frac{V_{DC}}{V_{PV}} * \frac{1}{LIR * I_B} \tag{3.10}$$

Where,

f : switching frequency of the buck converter

LIR : inductor current ratio expressed as a percentage of I_B

3.4 Battery Modeling

Lithium-ion battery model has been considered in this work for its higher efficiency and cycle life compared to the conventional lead-acid batteries [50]. Although different kinds of electrical equivalent model of battery are found in the literature, most of them fall within three types: Thevenin, impedance, and runtime based models. However, any of these models alone cannot predict I-V and runtime performance precisely in the simulation environment. The simplest Thevenin based model with a series resistor and a parallel RC network unable to predict battery runtime. Although its derivative model [51] can predict runtime, it suffers from error and high complexity. Impedance based models works with particular temperature and state of charge

(SoC) which fails to predict battery runtime [52]. Complex runtime based model [53] can simulate DC voltage response and battery runtime for a fixed discharge current. However, it fails to predict voltage response and runtime for varying load currents. To overcome these problem the battery model considered here is a combination of features of aforementioned three basic electrical models [54]. The nonlinear electrical battery model is shown in Figure 3.4 [54]. In this model, $V_{Batt,}$ I_{Batt} and V_{OC} stands for battery output voltage, output current and open circuit voltage respectively. R_{Series} characterize instantaneous voltage drop of the battery. The RC networks (R_{T_S} , C_{T_S}) and (R_{T_L} , C_{T_L}) represent the short term and long term time constants of battery step response respectively.

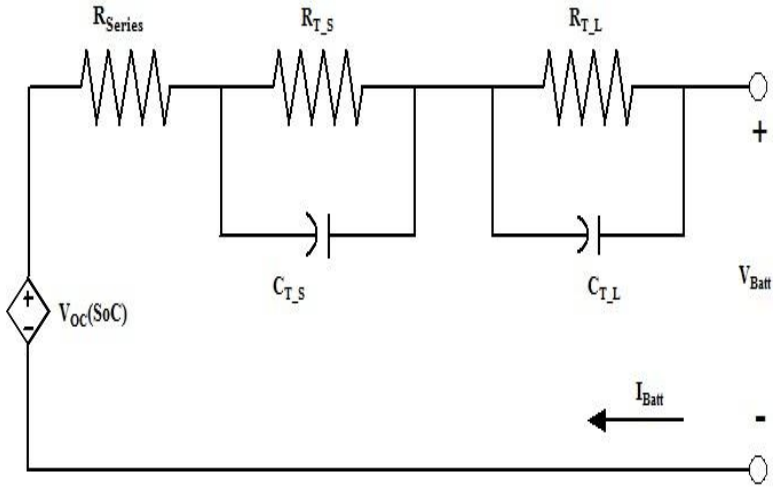

Figure 3.4 : Electrical equivalent circuit of battery

All the non-linear circuit parameters of the battery model presented above are function of state of charge (SoC) of the battery and can be represented mathematically as follows [54]:

$$V_{OC}\left(SoC\right) = 3.685 + 0.2156\left(\mathrm{SoC}\right) - 1.031e^{-35(SoC)} - 0.1178\left(\mathrm{SoC}\right)^2 + 0.3201\left(\mathrm{SoC}\right)^3 \qquad (3.11)$$

$$R_{Series}\left(SoC\right) = 0.07446 + (0.1562)2^{-24.37(SoC)} \qquad (3.12)$$

$$R_{T\_S}(SoC) = 0.04669 + (0.3208)e^{-29.14(SoC)} \tag{3.13}$$

$$C_{T\_S}(SoC) = 703.6 + (-752.9)e^{-13.51(SoC)} \tag{3.14}$$

$$R_{T\_L}(SoC) = 0.04984 + (6.603)e^{-155.2(SoC)} \tag{3.15}$$

$$C_{T\_L}(SoC) = 4475 + (-6056)e^{-27.12(SoC)} \tag{3.16}$$

3.5 Modeling of Bidirectional Buck-Boost Converter for ESS

Both battery and supercapacitor energy storage devices are connected to the DC bus through bi-directional buck boost converter. The topology of the bi-directional buck-boost converter is shown in Figure 3.5. During buck mode the bidirectional converter charges the energy storage from DC link in one direction and transfers energy to the DC link capacitor in the other direction during boost mode. IGBTs are used as the switching devices in the circuit. The operation of the converter depends on the terminal voltage of the storage device and the DC link voltage. The main purpose of the bidirectional buck-boost converter is to regulate the DC link voltage at a certain reference value by charging or discharging. The inductor L_{ST} is designed from the boost mode using following equations [55].

$$V_{DC} = \frac{V_{ST}}{1-d} \tag{3.17}$$

The inductor ripple current when switch S_1 is on is:

$$\Delta I_{LSC(on)} = (\frac{V_{ST}}{L_{ST}})T_{on} \tag{3.18}$$

And when it is off,

$$\Delta I_{LST(off)} = (\frac{V_{ST} - \frac{V_{ST}}{1-d}}{L_{ST}})T_{off} \tag{3.19}$$

At steady state, $\Delta I_{LST(on)} = \Delta I_{LST(off)}$ and $T = T_{on} + T_{off} = 1/f_s$

$$\Delta I_{LST} = \frac{V_{ST}}{L_{ST}} dT \quad or \quad L_{ST} = \frac{V_{ST} dT}{\Delta I_{LST}} \tag{3.20}$$

Where,

V_{DC} : DC link voltage

V_{ST} : voltage across energy storage device

d : duty of the buck boost converter IGBT

$\Delta I_{LST(on)}$: inductor ripple current when S_1 is on

$\Delta I_{LST(off)}$: inductor ripple current when S_1 is off

T_{on} : IGBT on period

T_{off} : IGBT off period

T : switching period

f_s : switching frequency

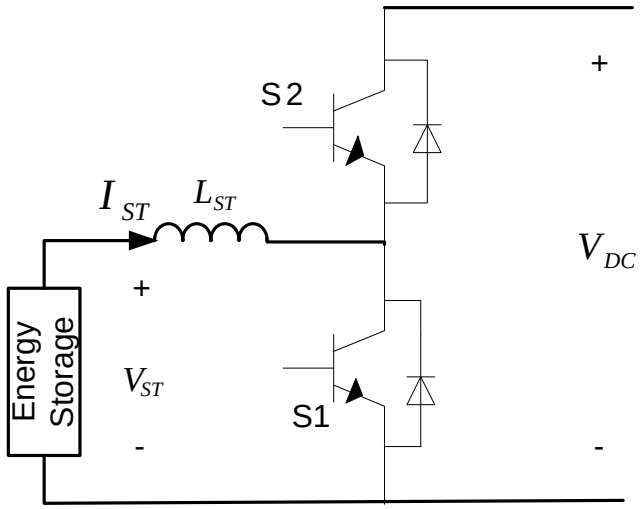

Figure 3.5 : Bidirectional buck boost converter for energy storage

3.6 Modeling of Voltage Source Converter

The topology of three phase bidirectional voltage source converter is shown in Figure 3.6. The converter has six semiconductor switches (S_1-S_6) and it is connected to the AC side through interface reactor having inductance L_s and resistance R_s. The DC link capacitor C_{DC} is connected to the DC side to smooth out the DC bus voltage. The power flow through the converter is controlled by proper switching of the semiconductor switches.

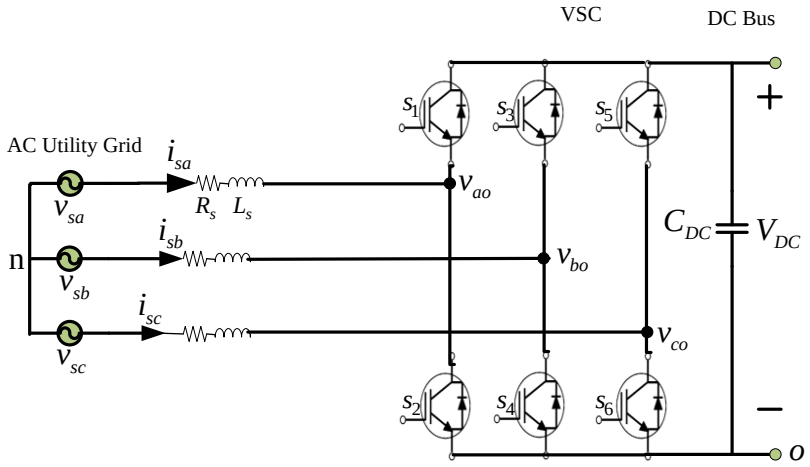

Figure 3.6 : Bidirectional voltage source converter

The switches of the converter of each leg are operated in complementary fashion in order to avoid short circuit. The switching signals S_a, S_b and S_c are related with the switching states in the following manner

$$S_a = \begin{cases} 1 \text{ if } S_1 \text{ is ON and } S_2 \text{ is OFF} \\ 0 \text{ if } S_1 \text{ is OFF and } S_2 \text{ is ON} \end{cases} \tag{3.21}$$

$$S_b = \begin{cases} 1 \text{ if } S_3 \text{ is ON and } S_4 \text{ is OFF} \\ 0 \text{ if } S_3 \text{ is OFF and } S_4 \text{ is ON} \end{cases} \tag{3.22}$$

$$S_c = \begin{cases} 1 \text{ if } S_5 \text{ is ON and } S_6 \text{ is OFF} \\ 0 \text{ if } S_5 \text{ is OFF and } S_6 \text{ is ON} \end{cases} \quad (3.23)$$

The output voltage depends on the switching signals as follows

$$v_{ao} = S_a V_{DC} \quad (3.24)$$

$$v_{bo} = S_b V_{DC} \quad (3.25)$$

$$v_{co} = S_c V_{DC} \quad (3.26)$$

Where, v_{ao},v_{bo} and v_{co} are the phase to neutral voltage of the converter.

The output voltage vector can be written as

$$\vec{v} = \frac{2}{3}(v_{ao} + pv_{bo} + p^2 v_{co}) \quad (3.27)$$

Where, $p = e^{j\frac{2\pi}{3}} = -\frac{1}{2} + j\frac{\sqrt{3}}{2}$ is a unitary vector representing 120^0 phase displacement between phases.

For three switching signals S_a, S_b and S_c there are eight switching states generating eight voltage vectors as shown in Table 3.1. It is seen that two voltage vectors (V_0 and V_7) being identical results only seven different voltage vectors.

The bidirectional converter operates in two modes: rectification and inversion mode. In rectification mode power is transferred from AC side to DC side whereas in inversion mode power flows from DC bus to the AC side. The load current dynamics for both mode of operation is derived here.

Table 3.1 : Switching states and voltage vectors of VSC

Switching States			Space Voltage Vector
S_a	S_b	S_c	V
0	0	0	$V_0 = 0$
0	1	0	$V_1 = \frac{2}{3}V_{DC}$
1	1	0	$V_2 = (\frac{1}{3} + j\frac{\sqrt{3}}{3})V_{DC}$
0	1	0	$V_3 = (-\frac{1}{3} + j\frac{\sqrt{3}}{3})V_{DC}$
0	1	1	$V_4 = -\frac{2}{3}V_{DC}$
0	0	1	$V_5 = (-\frac{1}{3} - j\frac{\sqrt{3}}{3})V_{DC}$
1	0	1	$V_6 = (\frac{1}{3} - j\frac{\sqrt{3}}{3})V_{DC}$
1	1	1	$V_7 = 0$

(a) Rectification mode

In this mode power flows from three phase AC side to the DC side. By applying Kirchhoff's voltage law to each phase of the AC supply side we get,

$$v_{sa} = L_s \frac{di_{sa}}{dt} + R_s i_{sa} + v_{ao} - v_{no} \tag{3.28}$$

$$v_{sb} = L_s \frac{di_{sb}}{dt} + R_s i_{sb} + v_{bo} - v_{no} \tag{3.29}$$

$$v_{sc} = L_s \frac{di_{sc}}{dt} + R_s i_{sc} + v_{co} - v_{no} \tag{3.30}$$

According to space vector definition, the voltage and currents can be expressed as follows

$$\vec{v}_s = \frac{2}{3}(v_{sa} + pv_{sb} + p^2 v_{sc}) \tag{3.31}$$

$$\vec{i}_s = \frac{2}{3}(i_{sa} + pi_{sb} + p^2 i_{sc}) \tag{3.32}$$

$$\vec{v} = \frac{2}{3}(v_{ao} + pv_{bo} + p^2 v_{co}) \tag{3.33}$$

$$\vec{v}_n = \frac{2}{3} v_{no}(1 + p + p^2) = 0 \tag{3.34}$$

Now, in terms of the space vectors, the AC system current dynamics can be written as

$$\vec{\mathrm{v}}_s = L_s \frac{d\vec{i}_s}{dt} + R_s \vec{i}_s + \vec{\mathrm{v}} \tag{3.35}$$

The voltage vector of the converter $\vec{\mathrm{v}}$ is related with the dc link voltage and switching state vector $\vec{S}_w$ by following relation

$$\vec{v} = \vec{S}_w V_{DC} \tag{3.36}$$

$$\vec{S}_w = \frac{2}{3}(S_a + pS_b + p^2 S_c) \tag{3.37}$$

The equation (3.35) can be rewritten in the following form

$$\frac{d\vec{i}_s}{dt} = -\frac{R_s}{L_s}\vec{i}_s + \frac{1}{L_s}(\vec{v}_s - \vec{v}) \tag{3.38}$$

(b) Inversion mode

In this mode power flows from DC side to the AC grid. The load current dynamics for inverter mode of operation can be obtained following the same way as in rectification mode and given by following expression

$$\frac{d\vec{i}_s}{dt} = -\frac{R_s}{L_s}\vec{i}_s + \frac{1}{L_s}(\vec{v} - \vec{v}_s) \tag{3.39}$$

3.7 Control Objective

The main objective of the power management control strategy is to ensure power balance among different modules of the microgrid. Since the power generation from the renewable sources is unpredictable it is more likely to create instability in the microgrid. In this work a decentralized control strategy has been used for autonomous operation of the microgrid. The advantage of the proposed control technique is that it does not require any centralized controller and communication system and thus, increases the system reliability.

3.8 Proposed Control Strategy

Since the interconnections of microgrid with the utility grid as well as the different modules of microgrid subsystem are made through power electronic interfaces, the effectiveness of any energy management strategy depends on the proper control of these power electronic converters. Following sub-sections illustrate the implemented control strategy for interfacing power converters.

3.8.1 Proposed Model Predictive Control of the Bidirectional VSC

Different control techniques for grid side voltage source converter have been adopted such as synchronous reference frame based P-Q control [37] [56], direct power control (DPC) [57]–[59], fuzzy logic control [60], sliding mode control (SMC) [61], internal model control (IMC)-based control [62]. In this work model predictive controller has been used to control the grid voltage source converter. The application of model predictive control (MPC) for controlling power converter is gaining popularity compared to the classical controllers due to its simplicity and easy implementation [63], faster dynamic response and easy inclusion of constraints and

non-linearity. Another important advantage of the MPC compared to the classical controller is that it does not require any pulse width modulator [64].

In this work, finite control set model predictive control (FCS-MPC) has been proposed to control the power flow through VSC. The reference power for the VSC controller comes from grid operator during normal operating mode and from voltage regulator (K_v) when DC bus voltage is controlled by main grid. The control architecture is shown in Figure 3.7. The MPC algorithm takes advantages of discrete characteristic and finite set of switching pattern of the power electronic converters.

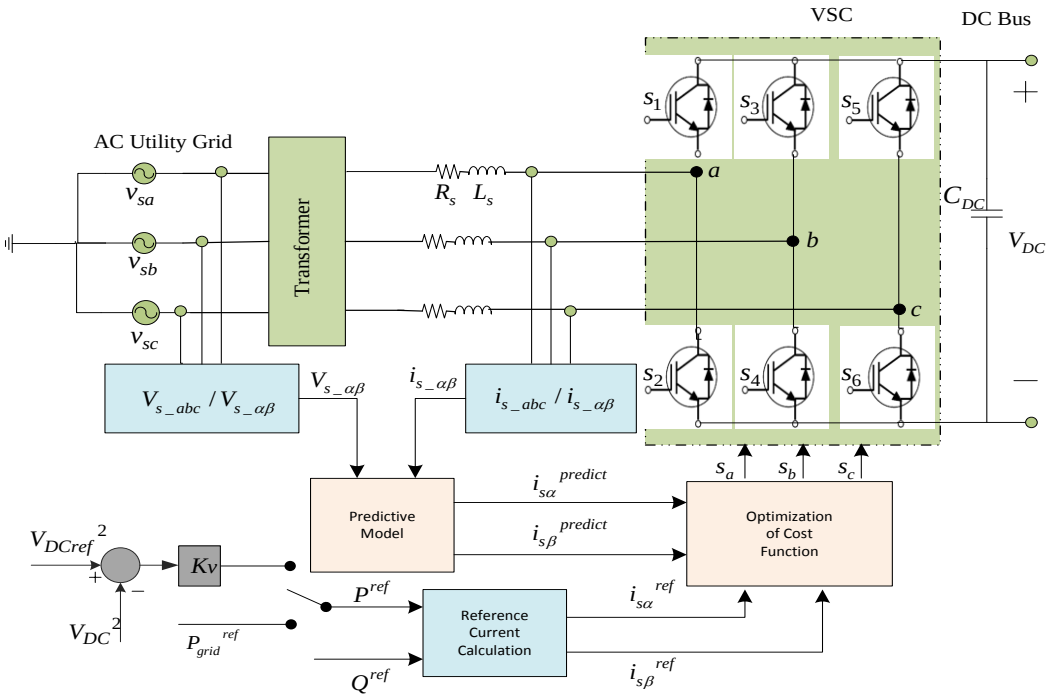

Figure 3.7 : Control architecture of VSC

To formulate the MPC algorithm, a discrete time model of power converter is required. The discrete system model is used to predict the future input current for $(m+1)^{th}$ sampling instant

based on the measured input current, grid voltage vector and converter voltage vector at m^{th} sampling instant. The discrete time model has been obtained by approximating the input current derivative using forward Euler approximation for a sampling time of T_s as given below.

$$\frac{d\vec{i}_s}{dt} \approx \frac{\vec{i}_s(m+1) - \vec{i}_s(m)}{T_s} \tag{3.40}$$

The predicted input current at $(m+1)^{th}$ sampling instant for rectification and inverting mode can be expressed as follows

$$\vec{i}_{s\_rec}^{\,predict}(m+1) = (1 - \frac{R_s T_s}{L_s})\vec{i}_{s\_rec}(m) + \frac{T_s}{L_s}[\vec{v}_s(m) - \vec{v}(m)] \tag{3.41}$$

$$\vec{i}_{s\_inv}^{\,predict}(m+1) = (1 - \frac{R_s T_s}{L_s})\vec{i}_{s\_inv}(m) + \frac{T_s}{L_s}[\vec{v}(m) - \vec{v}_s(m)] \tag{3.42}$$

During real time implementation of MPC if the computation time is larger than the sampling time a delay will occur between the time of current measurement and actuation of new switching states. This delay will result in oscillation of converter load current around its reference value. To overcome this problem delay compensation has been included which predicts the current by shifting load model one step forward in time [65]. After delay compensation predicted current becomes as follows

$$\vec{i}_{s\_rec}^{\,predict}(m+2) = (1 - \frac{R_s T_s}{L_s})\vec{i}_{s\_rec}(m+1) + \frac{T_s}{L_s}[\vec{v}_s(m+1) - \vec{v}(m+1)] \tag{3.43}$$

$$\vec{i}_{s\_inv}^{\,predict}(m+2) = (1 - \frac{R_s T_s}{L_s})\vec{i}_{s\_inv}(m+1) + \frac{T_s}{L_s}[\vec{v}(m+1) - \vec{v}_s(m+1)] \tag{3.44}$$

Transforming the voltage and current vectors into α-β reference frame the predicted input current can be written in the α-β co-ordinate as $i_{s\alpha}^{\,predict}$ *and* $i_{s\beta}^{\,predict}$.

The basis of selecting optimum switching state in MPC is to minimize the error between reference variables and predicted variables. Therefore, a cost function J incorporating the predictive current and reference current is formulated. The cost function is expressed as the absolute error between reference and predicted current as follows

$$J = \left| i_{s\alpha}^{\ ref} - i_{s\alpha}^{\ predict} \right| + \left| i_{s\beta}^{\ ref} - i_{s\beta}^{\ predict} \right| \tag{3.45}$$

Minimize J

The reference current in α-β reference frame is computed from direct axis and quadrature axis reference currents obtained from following equations

$$i_d^{\ ref} = \frac{2}{3V_d} P^{ref} \tag{3.46}$$

$$i_q^{\ ref} = -\frac{2}{3V_d} Q^{ref} \tag{3.47}$$

Where, V_d is the direct axis component of AC grid voltage; P^{ref} is the reference real power and Q^{ref} is the reference reactive power. The steps of MPC are presented in the flow chart as shown in Figure 3.8.

ESS remains in floating/charging mode when DC bus voltage is dominated by VSC. Reference power is generated by a lead-lag controller based outer voltage regulator. The voltage regulator has been designed based on the DC voltage dynamics deduced from following power balance equation [66].

$$P_{load} + \frac{d}{dt}\left(\frac{1}{2} C V^2_{DC}\right) + P_{grid} = P_{PV} \tag{3.48}$$

Where, P_{load}, P_{grid} and P_{PV} are the load power, grid demand and PV power respectively. Voltage regulator has been designed by considering the load power and PV power as disturbance input.

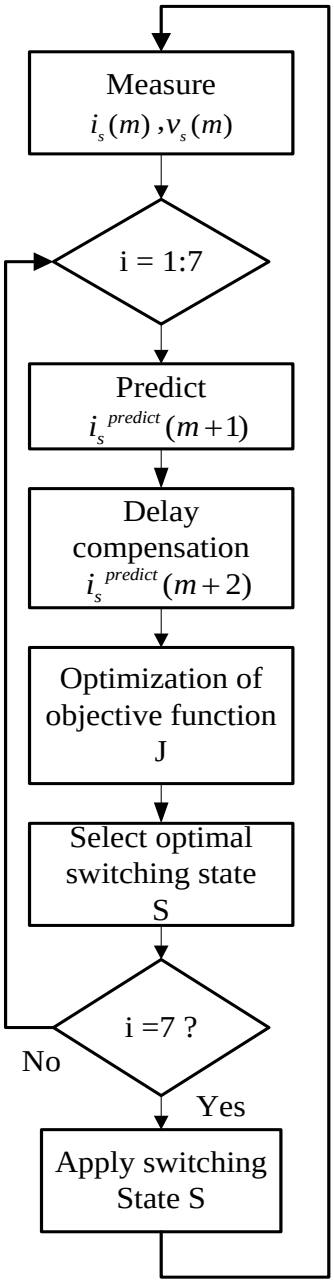

Figure 3.8 : Flow chart of MPC for two level VSC

3.8.2 Control of the Bidirectional DC-DC Converter for ESS

For interfacing storage devices to the common DC bus use of both isolated and non-isolated bidirectional DC-DC converter have been reported [67]. In this work, non-isolated bidirectional buck-boost converter has been used for its simpler design and better efficiency. The bidirectional buck-boost converter controls the DC bus voltage by charging/discharging energy storage. Two cascaded PI controllers serve the control objective. The reference current produced from outer voltage control loop is supplied to the low pass filter (LPF) to divide the reference current between battery and supercapacitor. Same control strategy has been adopted for battery and supercapacitor. The control architecture is shown in Figure 3.9.

During boost mode, the converter switch S_1 is on and S_2 is off and energy storage is discharged and the opposite is true for buck mode of the converter. Converter model for buck mode is given in equation (3.49).

$$V_L = L\frac{di_L}{dt} = DV_{DC} - V_{st} \tag{3.49}$$

Where, D, V_L, i_L , and V_{st} denotes the control variable, inductor voltage drop, inductor current and terminal voltage of storage device respectively.

Inverse model control of buck-boost converter is used here [68]. In this mode of control, the target is to establish the equality between regulator output and voltage drop in the inductor. The linearization of the converter gives the transfer function as below

$$G_i(s) = \frac{I_L(s)}{V_L(s)} = \frac{1}{L.s} \tag{3.50}$$

Transfer function of the inner current control loop without a filter is given by

$$F_i(s) = \frac{PI_I(s).G_i(s)}{1 + PI_I(s).G_i(s)} = \frac{K_{pI}.s + K_{iI}}{L.s^2 + K_{pI}.s + K_{iI}} \tag{3.51}$$

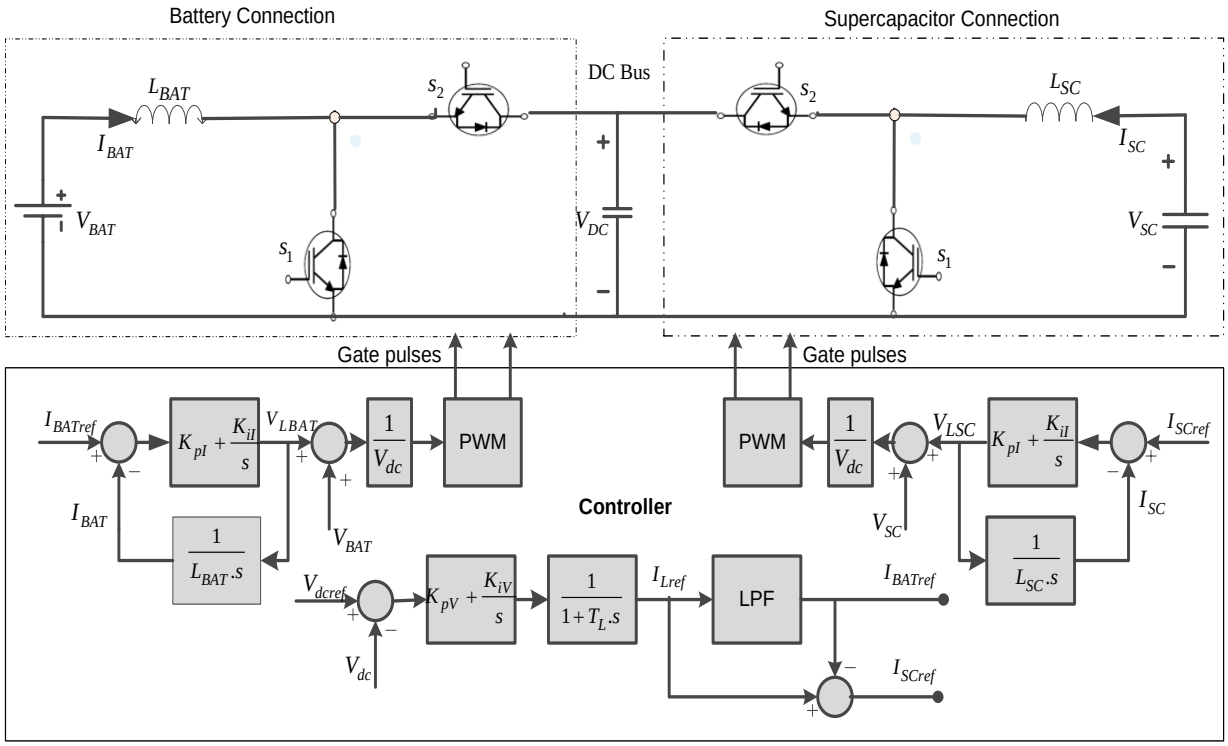

Figure 3.9: Control architecture of ESS

To ensure dynamics control a filter is used for reference current of inductor [68]. Then the closed loop transfer function becomes

$$F_{if}(s) = \frac{I_L(s)}{I_{Lref}(s)} = \frac{1}{1+T_L.s} \cdot \frac{1+\frac{K_{pI}}{K_{iI}}s}{\frac{L}{K_{iI}}s^2 + \frac{K_{pI}}{K_{iI}}.s+1} \tag{3.52}$$

The simplified transfer function is obtained as

$$F_{if}(s) = \frac{I_L(s)}{I_{Lref}(s)} = \frac{1}{\frac{L}{K_{iI}}s^2 + \frac{K_{pI}}{K_{iI}}.s+1} \tag{3.53}$$

$$T_L(s) = \frac{K_{pI}}{K_{iI}} \tag{3.54}$$

The simplified transfer function is compared with the standardized second order transfer function given below

$$F_{if}(s) = \frac{I_L(s)}{I_{Lref}(s)} = \frac{1}{\frac{1}{\omega_{ni}^{\ 2}} s^2 + \frac{2\xi}{\omega_{ni}} s + 1} \tag{3.55}$$

Thus, the proportional and integral gain of the inner PI regulator are obtained as follows

$$\begin{aligned} K_{pI} &= 2\xi\omega_{ni}L \\ K_{iI} &= \omega_{ni}^{\ 2}L \end{aligned} \tag{3.56}$$

Where, ω_{ni} is the bandwidth of the inner current loop control which is bounded by the switching frequency (f_s) of the converter as given below

$$\omega_{ni} \le \frac{2\pi f_s}{10} \tag{3.57}$$

Outer PI regulator generates reference current for DC bus voltage control based on the power balance equation expressed as below where $P_{storage}$ denotes storage power

$$P_{load} + \frac{d}{dt}(\frac{1}{2}CV^2_{DC}) + P_{grid} \pm P_{storage} = P_{PV} \tag{3.58}$$

3.8.3 Control of the DC-DC Buck Converter

The PV array output depends on irradiation of the sun and the temperature which are varying in nature. The MPPT algorithm determines the PV output power each instant of time and modify the operating point to get the maximum available power. The buck converter controller generates the duty cycle to track the reference voltage generated from incremental conductance (IC) based MPPT algorithm.

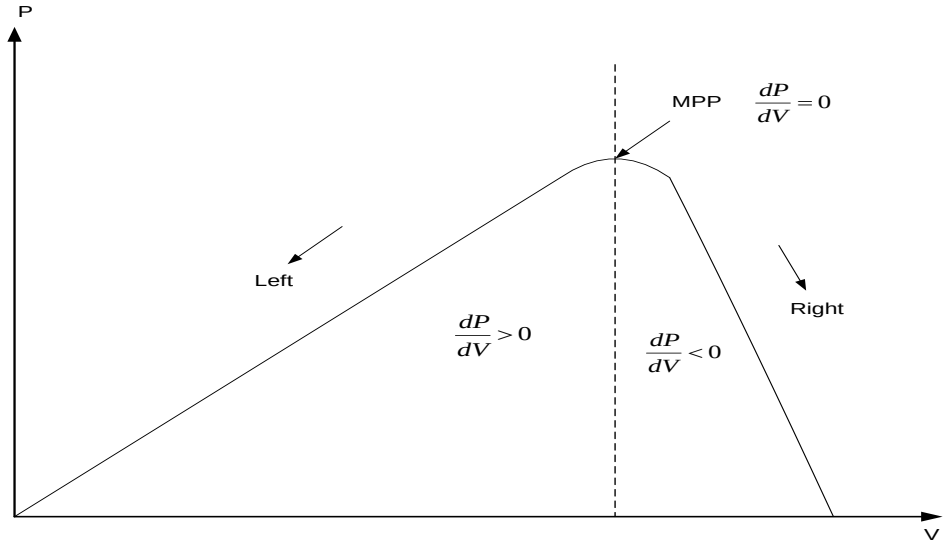

Figure 3.10: PV curve with MPP

The PV output power is given by

$$P_{PV} = I_{PV} V_{PV} \tag{3.59}$$

At the maximum operating point (MPP), the derivative of PV power is zero.

$$\frac{\partial P_{PV}}{\partial V_{PV}} = \frac{\partial (I_{PV} V_{PV})}{\partial V_{PV}} = 0 \tag{3.60}$$

The above equation can be reduced to the following form

$$\frac{\partial I_{PV}}{\partial V_{PV}} = -\frac{I_{PV}}{V_{PV}} \tag{3.61}$$

The input to the MPPT algorithm is PV output voltage and current; based on the equation (3.61) the IC algorithm generates the reference voltage (V_{ref}) for maximum PV output. The PV output voltage (V_{PV}) is compared with the reference voltage and the error is passed through a PI controller to generate the duty cycle of the buck converter. The structure of the buck converter controller is shown in Figure 3.11

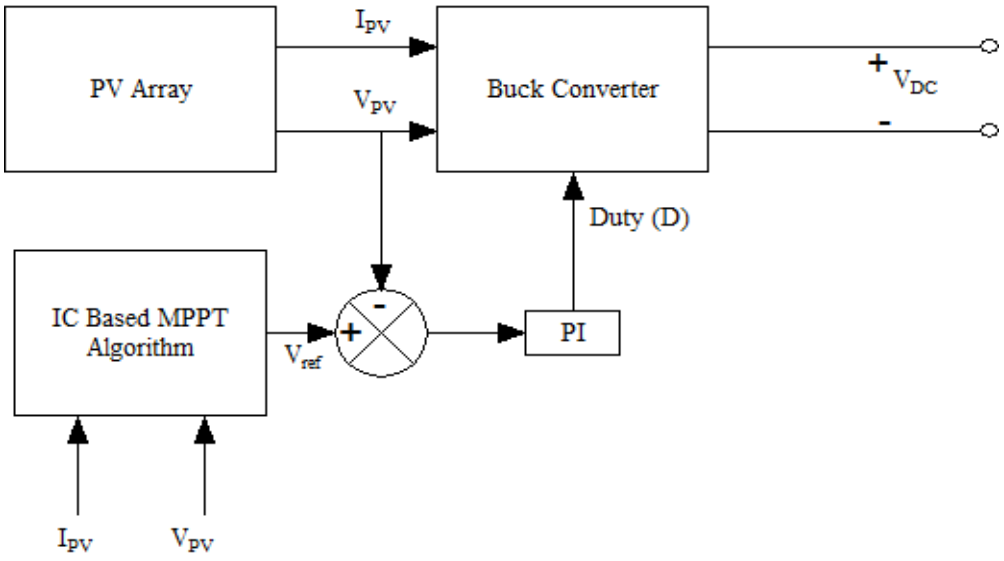

Figure 3.11: Buck converter controller

The output voltage of buck converter is given by

$$V_{DC} = DV_{PV} \tag{3.62}$$

The control signal D for the buck converter in Laplace domain can be expressed as

$$D = K_P V_{error} + \frac{K_I}{s} V_{error} \tag{3.63}$$

Where, $V_{error} = V_{ref} - V_{PV}$

K_P and K_I : are the PI regulator gains

CHAPTER 4

RESULTS AND DISCUSSIONS

4.1 Introduction

In order to investigate the performance of the proposed control strategy for the PV based DC microgrid, the control strategy and system model have been developed using RSCAD software and simulated using real time digital simulator (RTDS).

RTDS is a digital electromagnetic transient power system simulator which is capable of simulating complex power system network with faster speed and higher accuracy. RTDS works with its software package RSCAD. The comprehensive library and graphical user interface of the RSCAD software enables user to develop complex power system networks and their control systems. Since RTDS works in real time it produces system behavior that characterizes the response of a physical network. Another advantage of this simulator is that it can also be interfaced with physical devices. More details about RTDS can be obtained from its developer RTDS Technologies Inc [69].

4.2 Operating Strategy

Regarding operating strategy of the microgrid, both grid-connected and islanded mode of operation with different scenarios have been considered as given in Table 4.1. In the grid connected mode, microgrid delivers or receives power from the utility grid while maintaining all the power balance.

Table 4.1 : Microgrid Operating Modes

Mode	PV Status	ESS	VSC	Bus Voltage Control
Grid Connected (Day)	MPPT	Charging/discharging	Inverting mode	ESS
Grid Connected (Night)	Not Available	Floating/Charging	Rectifying mode	VSC
Islanded	MPPT	Discharging/charging	Disconnected	ESS

Two cases for grid-connected mode have been considered: day time operation and night time operation. During the period of day, PV works at maximum power point (MPP) and meets the demand of local load as well as demand sought from the main grid operator. To supply smooth power to the utility grid, the common DC bus voltage is controlled by the ESS by absorbing/supplying the power surplus/deficit. During night time, PV power becomes zero and microgrid receives power from the utility to meet the local demand. The dc bus voltage is regulated by the bidirectional VSC due to the uncertainty of the enough storage capacity of ESS. In this case, VSC works in the rectification mode and ESS remains floating or starts charging depending on the status of the charge. In case of islanded mode, the VSC is disconnected from microgrid. The PV still works in MPPT and microgrid enters into autonomous mode. ESS controls the DC bus voltage by charging/discharging depending on the PV output and local loads.

4.3 RTDS Implementation of the System

The system implementation includes both large time step (50 µsec) and small time step (2 µsec) components of RSCAD. The rating of the system parameters are presented in Table 4.2 and Table 4.3.

Table 4.2 : System Parameters

Parameters	Value
Utility grid voltage (V_s)	110 V (rms) phase to ground
DC link capacitance (C_{DC})	1000 µF
DC link voltage (V_{DC})	300 V
Reactor resistance (R_s)	0.1 Ω
Reactor inductance (L_s)	10 mH
Local load	1.8 kW
Sampling time (T_s)	50 µs
Lithium-ion Battery	100Ah/120 V
Supercapacitor module	125 V/5 F
PV panel	5.1 kW

Table 4.3 : Parameter of the PV Array

Parameter	Value
Open circuit voltage	21.7 V
Short circuit current	3.35 A
Voltage at P_{MAX}	17.4 V
Current at P_{MAX}	3.05 A
Series connected modules(N_{SS})	24
Parallel connected modules(N_{PP})	4
PV array voltage at P_{MAX}	417 V
PV array current at P_{MAX}	12.2 A
PV array maximum power	5.1 kW
Number of PV cells in each model	36
Ideality factor of PV diode, a	1.5
Temperature Dependency factor	3
Reference Temperature	25^{o}c
Temperature Coefficient of I_{SC}	0.065
Reference solar intensity	1000 W/m^2

The schematic of the DC microgrid as shown in Figure 4.1 is developed inside VSC bridge box using power system components of small time step library of RSCAD.

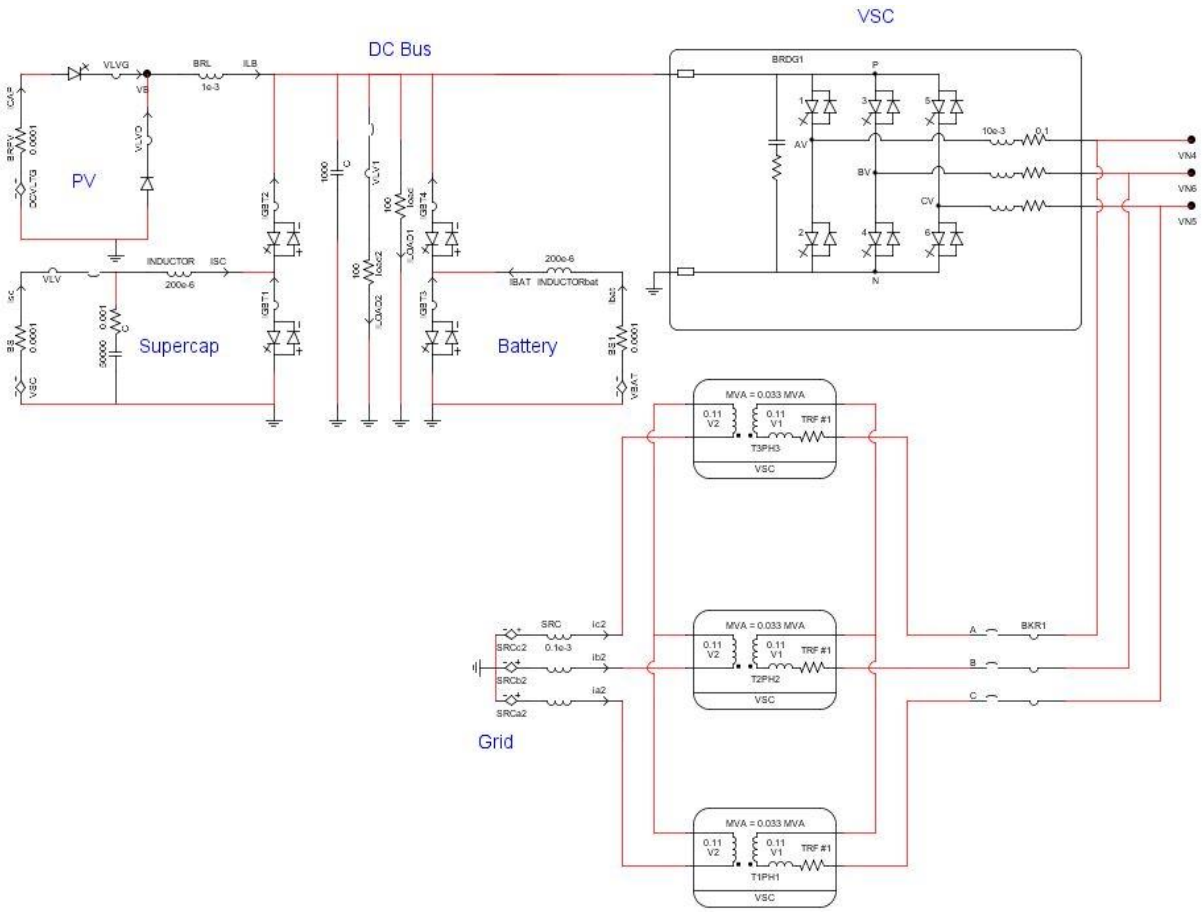

Figure 4.1 : Schematic of the system model

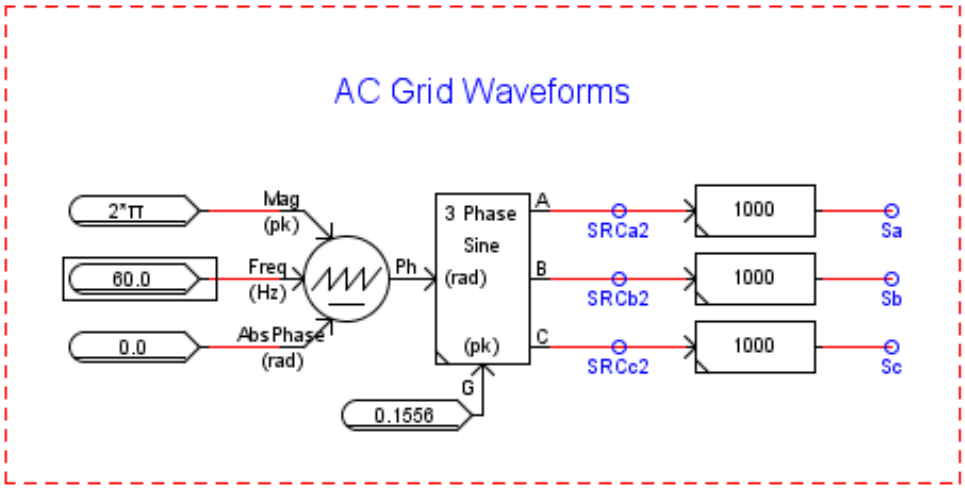

Figure 4.2 : Three phase grid voltage generation

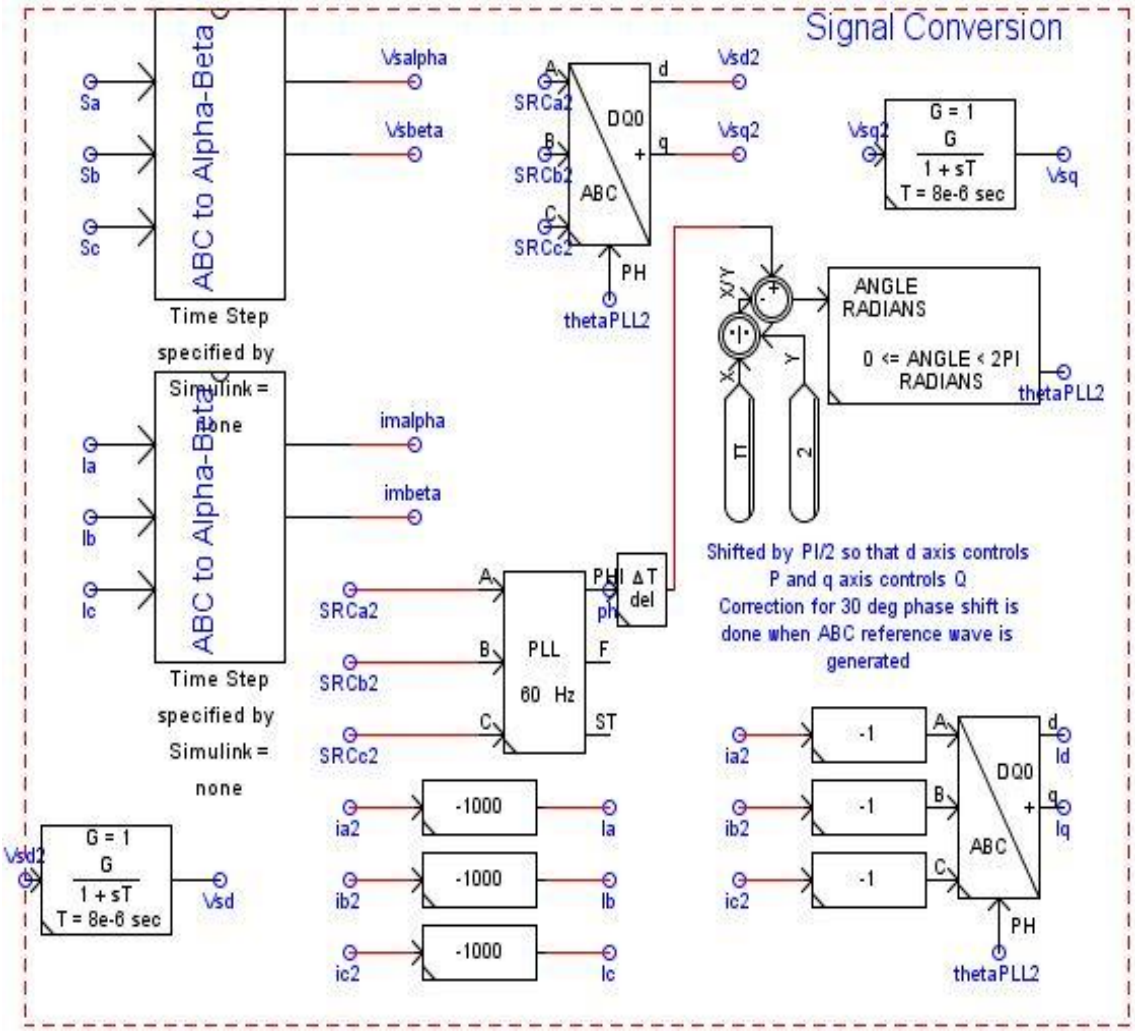

Figure 4.3 : Signal conversions

The control system is developed using large time step components of the RSCAD control library. The schematics of the MPC based VSC control, and buck-boost DC-DC converter controls for ESS are presented in Figure 4.2- Figure 4.5. The model predictive control algorithm is first developed using C programming and then tested in the MATLAB/Simulink environment. The control block named 'MPC Controller' as shown in Figure 4.4 is then built using 'component builder' feature of RSCAD which enables Simulink to RSCAD conversion.

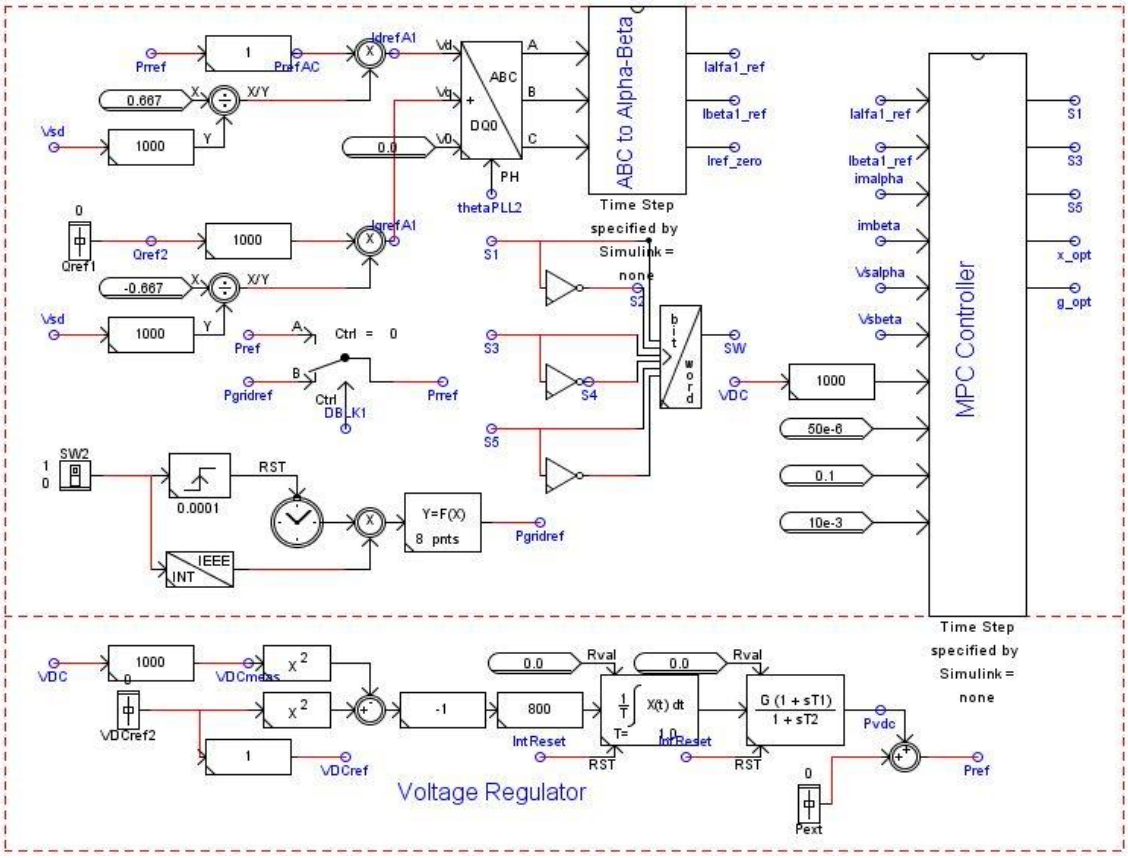

Figure 4.4 : Model predictive control of VSC

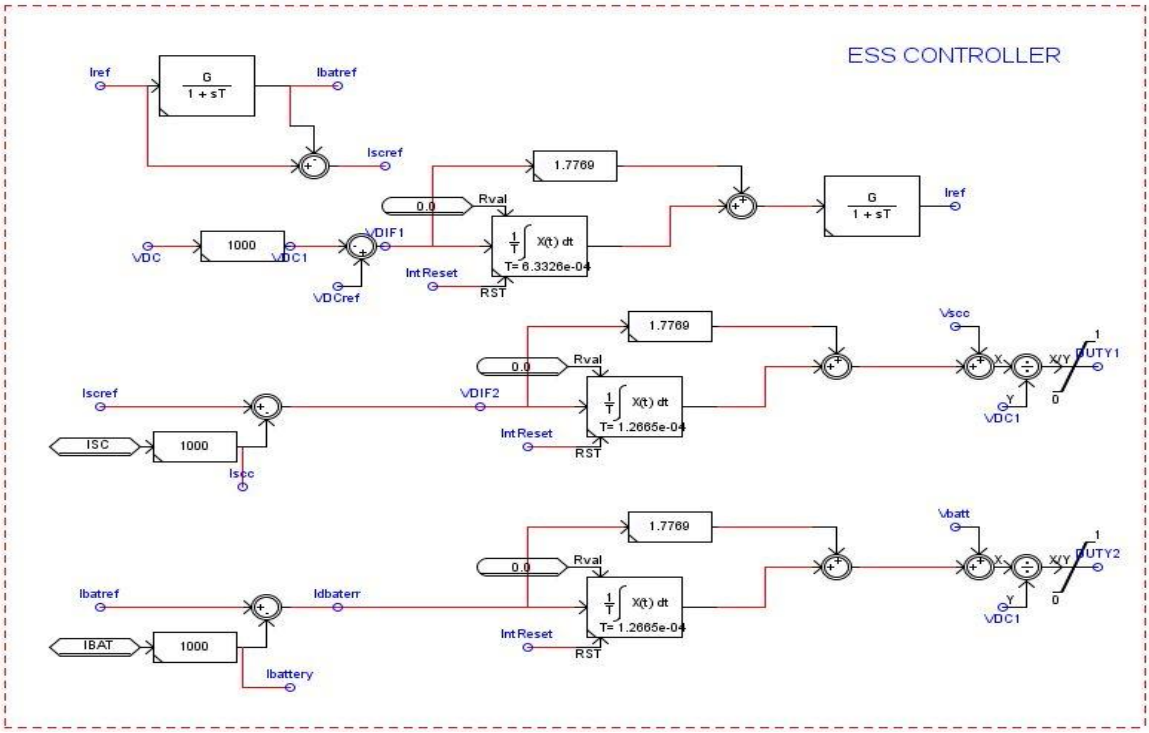

Figure 4.5 : Control of energy storage converters

4.4 RTDS Based Simulation Results and Discussions

During simulation study the local load of the microgrid has been assumed constant. The system is simulated for three different modes: grid connected (day), grid connected (night) and islanded as mentioned in Table 4.1. Different scenarios have been considered during each mode of simulation by changing PV power and grid power demand and possible mode transition.

The controller performance has been tested to control the DC bus voltage thus maintaining power balance in the DC side as well as power flow control with utility grid. The simulation results of different modes are shown below.

4.4.1 Grid Connected Mode (Day)

In this mode, the microgrid is connected to the utility grid and ESS controls the DC bus voltage. Microgrid meets the reference power sought by the grid operator while maintaining the local load. ESS charges/discharges when PV power is greater/less than the local load plus grid demand. The transients caused by the variation in the PV generation or grid reference power are absorbed by the supercapacitor. Simulated results are shown in Figure 4.6.

The PV works in MPP and the local load remain constant at 1.80 kW as shown in Figure 4.6 (a). The sun irradiation is 700 W/m^2 which produces PV power of 4 kW which greater than the local load plus utility grid demand (1 kW). The excess power is stored in the battery by charging. At 2.08 seconds the reference power sought by grid operator increased to 2 kW which reduces the rate of charging of the battery. The transient caused by the sudden change in the grid reference power is suppressed by the supercapacitor with little fluctuation in the DC bus voltage as shown in Figure 4.6 (b). After 2 seconds, the PV power falls to 3.69 kW due to the reduction of the solar irradiation. At this case, battery starts discharging to meet the deficiency between generation and demand. Thus, ESS effectively plays its role of smooth power transfer through

VSC by suppressing transients and controlling the DC bus voltage. The performance of the MPC based VSC controller is also found satisfactory to track the reference power.

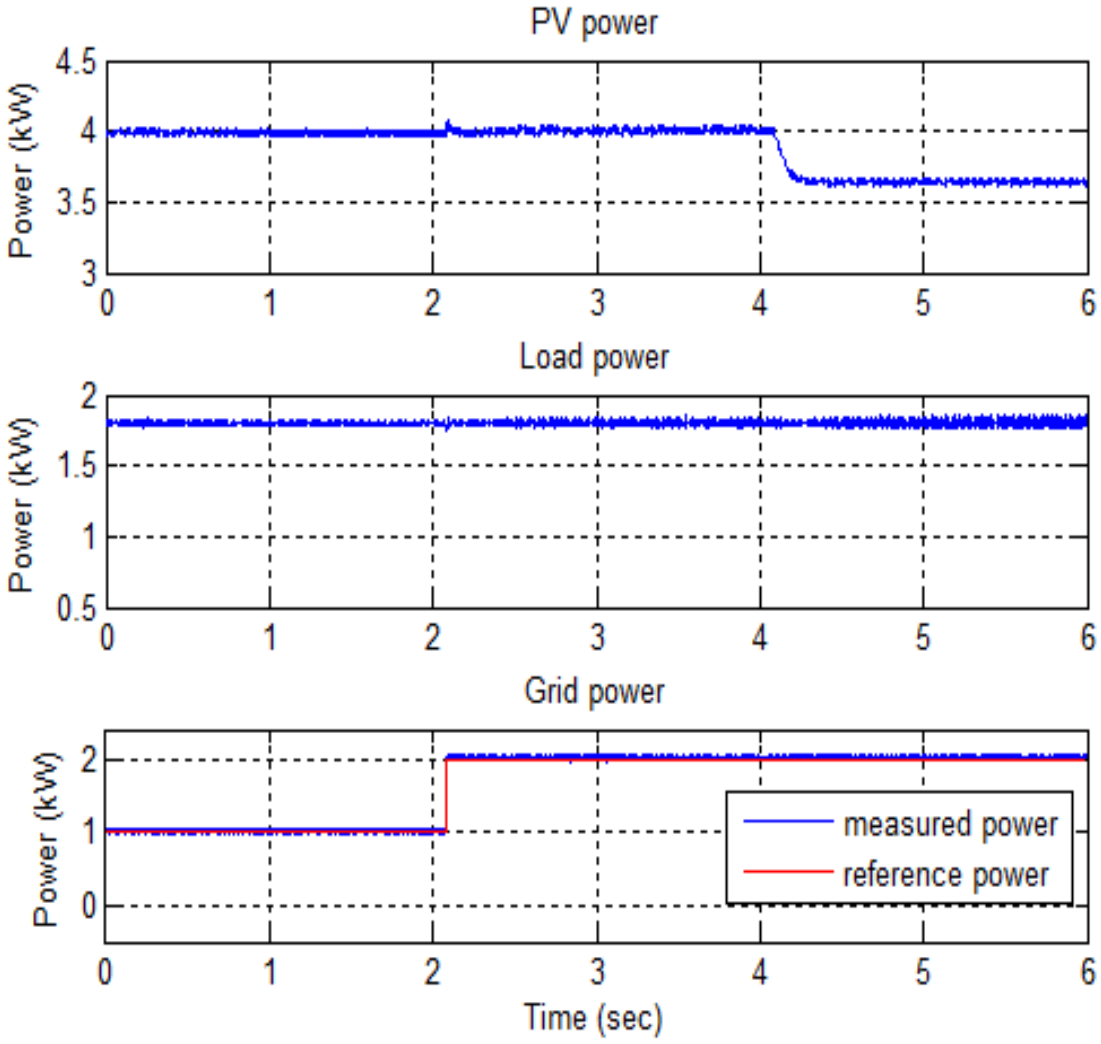

(a) Variation in PV power, load power and grid power

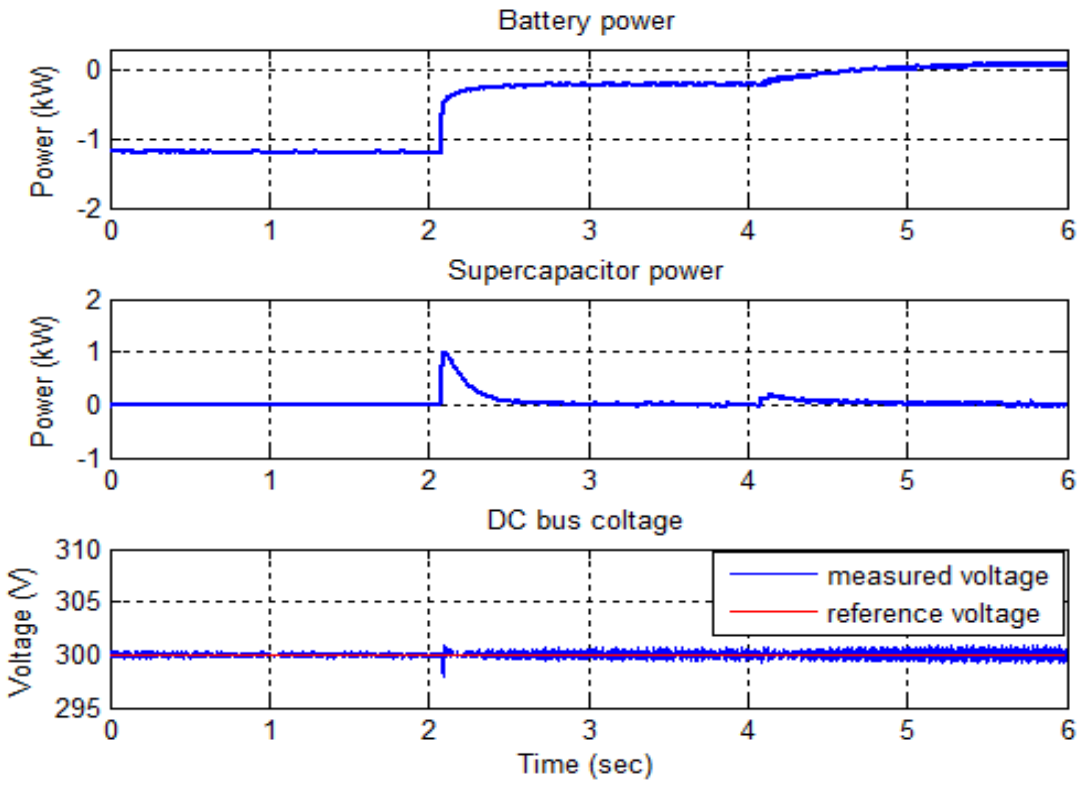

(b) Variation in battery power, supercapacitor power and DC bus voltage

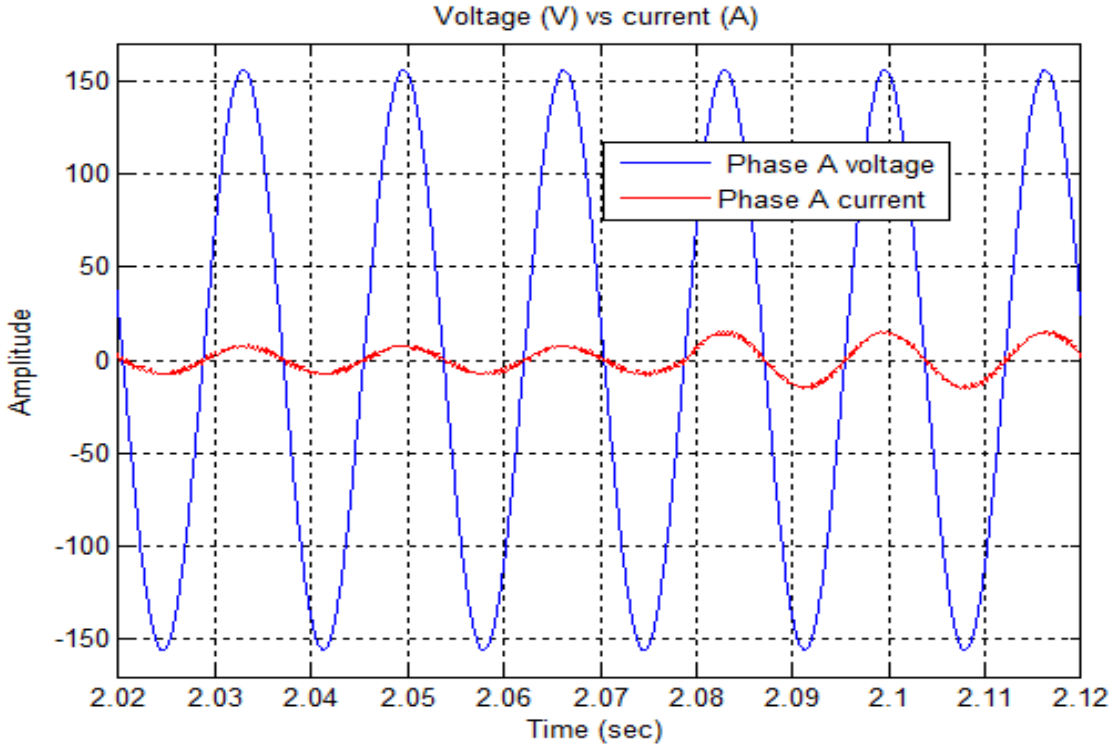

(c) Phase A voltage (phase to ground) and current variation

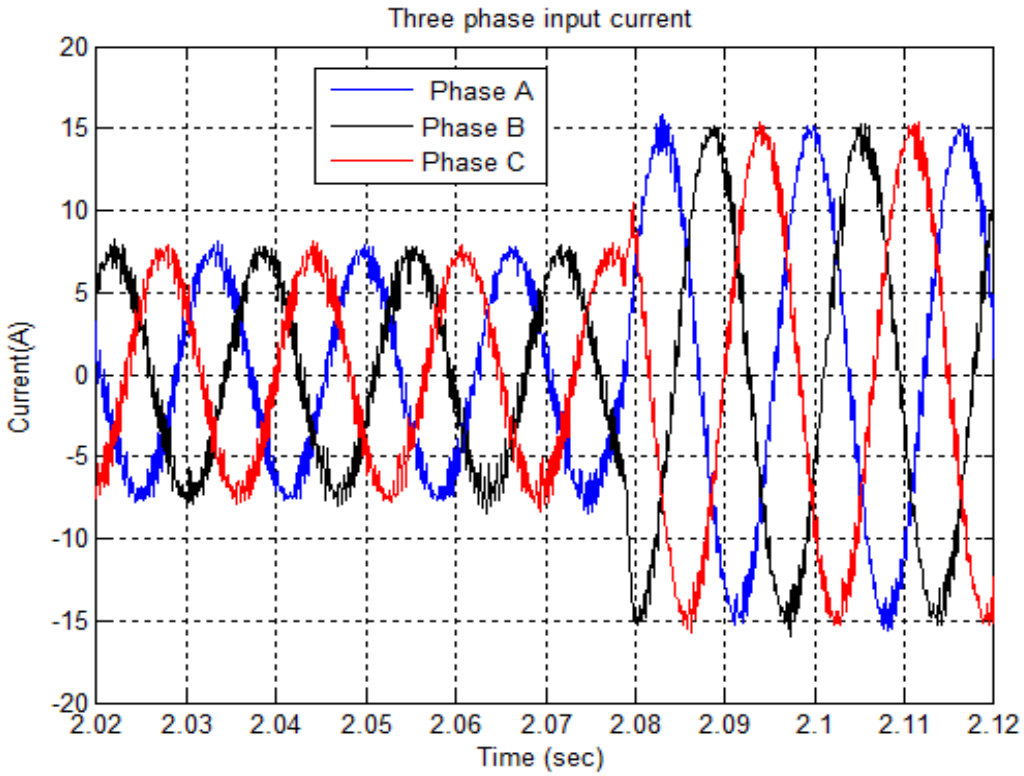

(d) Three phase input current variation

Figure 4.6 : Simulation of grid connected mode (day)

If the PV power is reduced during the cloudy day and at the same time load of the microgrid exceeds the aggregated capacity of PV and energy storage, there will be instability in the microgrid. The energy storage will no longer be able to support the DC link voltage. In this worst case the voltage source converter will regulate the DC bus voltage by importing power from utility grid to meet the power deficiency in the microgrid. The energy storage system will remain in the floating/charging mode in this case. Simulation results of this scenario are shown in Figure 4.7.

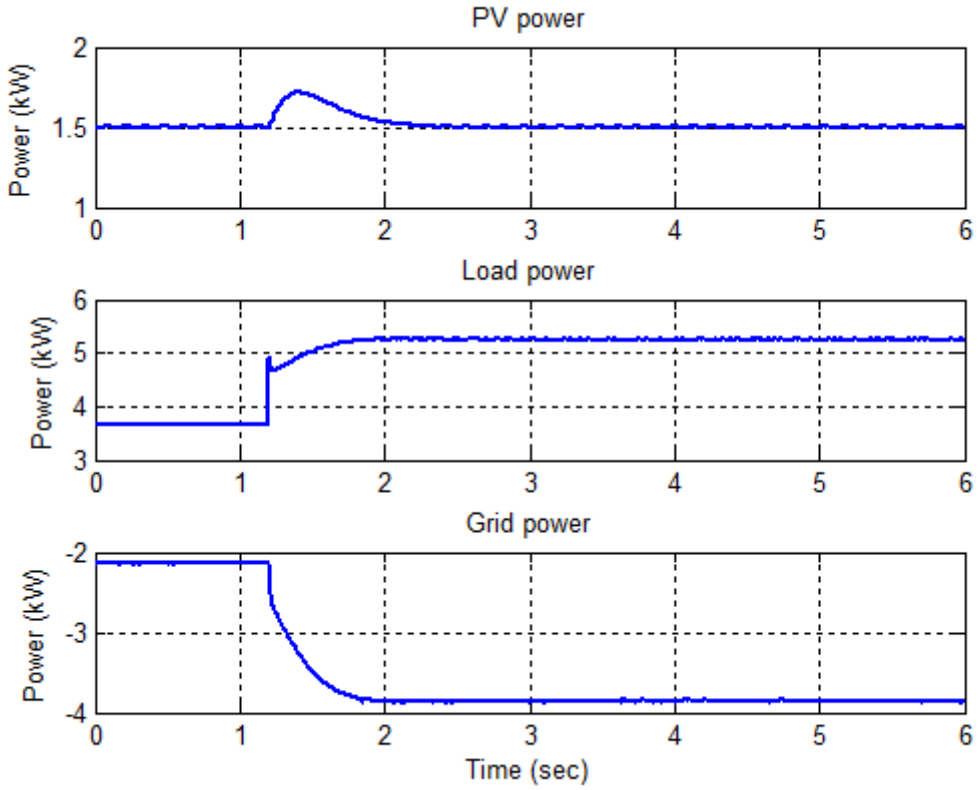

(a) Variation in PV power, load power and grid power

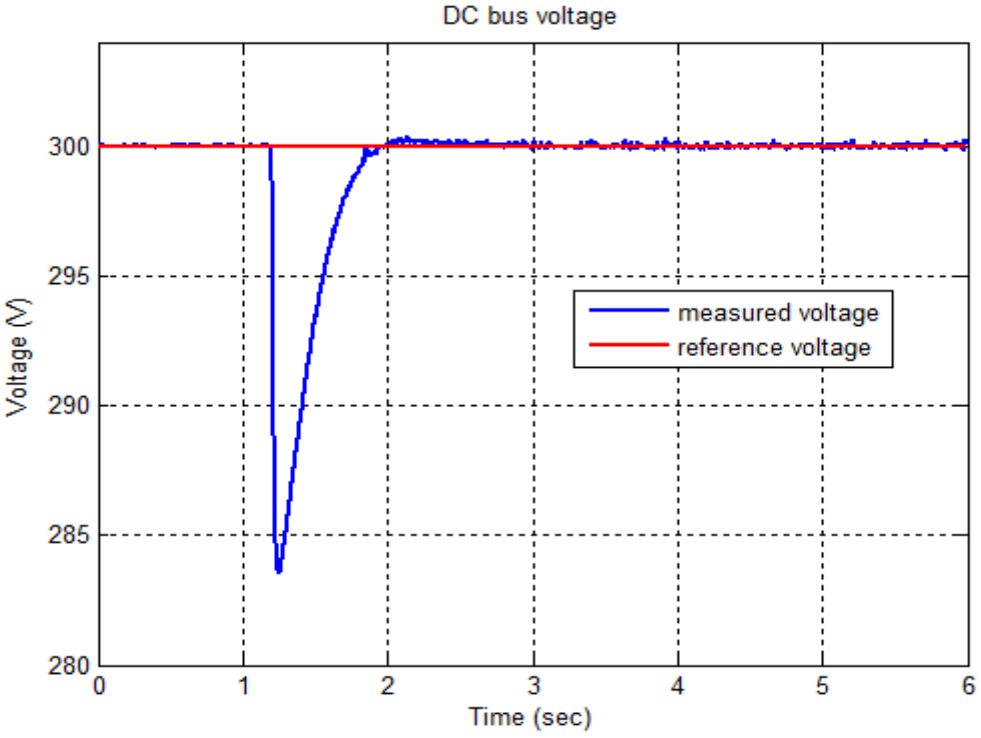

(b) Variation in DC bus voltage

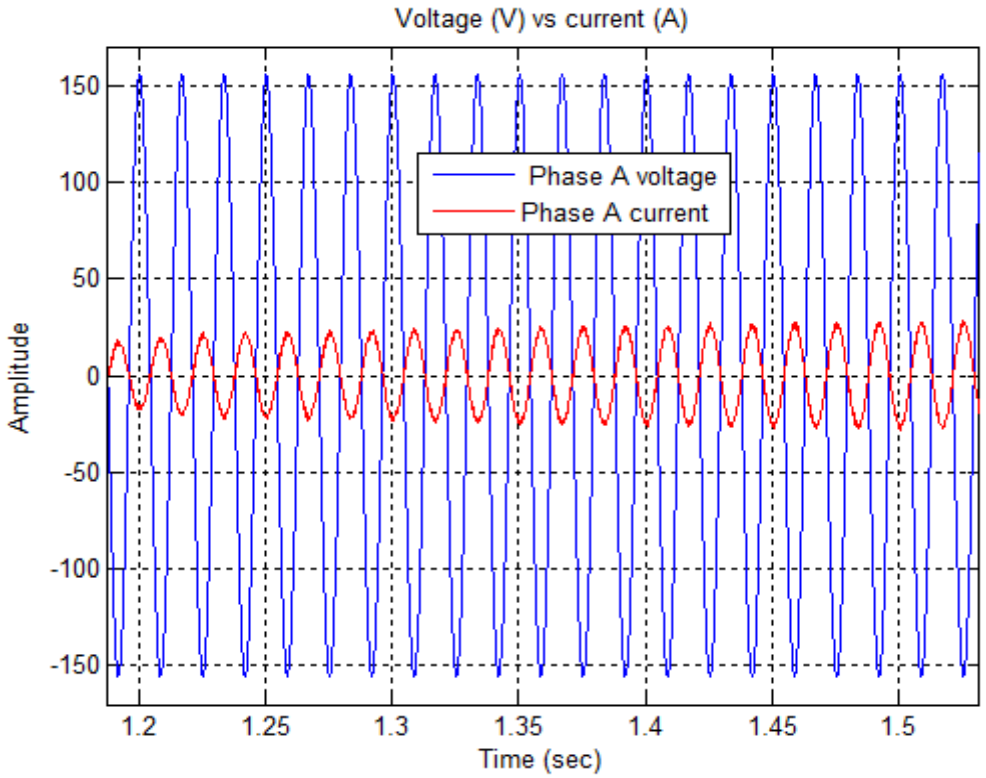

(c) Phase A voltage (phase to ground) and current variation

Figure 4.7 : Simulation of grid connected mode (day) with large increase in load

As shown in Figure 4.7 (a), the PV power is reduced to 1.5 kW and load is increased to 3.7 kW. The power mismatch is 2.2 kW which is greater than the nominal load (1.8 kW) of the microgrid. As capacity of energy storage device is set to be close to nominal load it can not support the power mismatch for the prolonged time. Therefore, power is drawn from the utility grid to meet the power deficit. The load power is again increased to 5.3 kW at 1.2 seconds which increases the power import from utility grid. The oscillation in the DC bus voltage due to load disturbance is shown in Figure 4.7 (b) which shows that voltage is well regulated with 5.5 percent variation. The relation between grid input current and voltage is 180 degree out of phase as shown in Figure 4.7 (c) which is opposite to the case of power exporting to the utility grid as shown in Figure 4.6 (c).

4.4.2 Islanded Mode

In this case, microgrid enters into islanded mode from grid connected mode. The power transfer between microgrid and main grid reduces to zero. Reconnection of the microgrid with the utility has also been simulated. The ESS regulates common DC bus voltage to the reference value. Power exchanged with utility grid, load, PV, battery and supercapacitor power are shown in Figure 4.8.

From Figure 4.8 (a) it is seen that islanding of the microgrid is triggered and after 1.0 second it is successfully reconnected to the main grid. The MPC controlled VSC strictly tracks the reference grid power before islanding (2 kW) and after reconnection (1.8 kW).

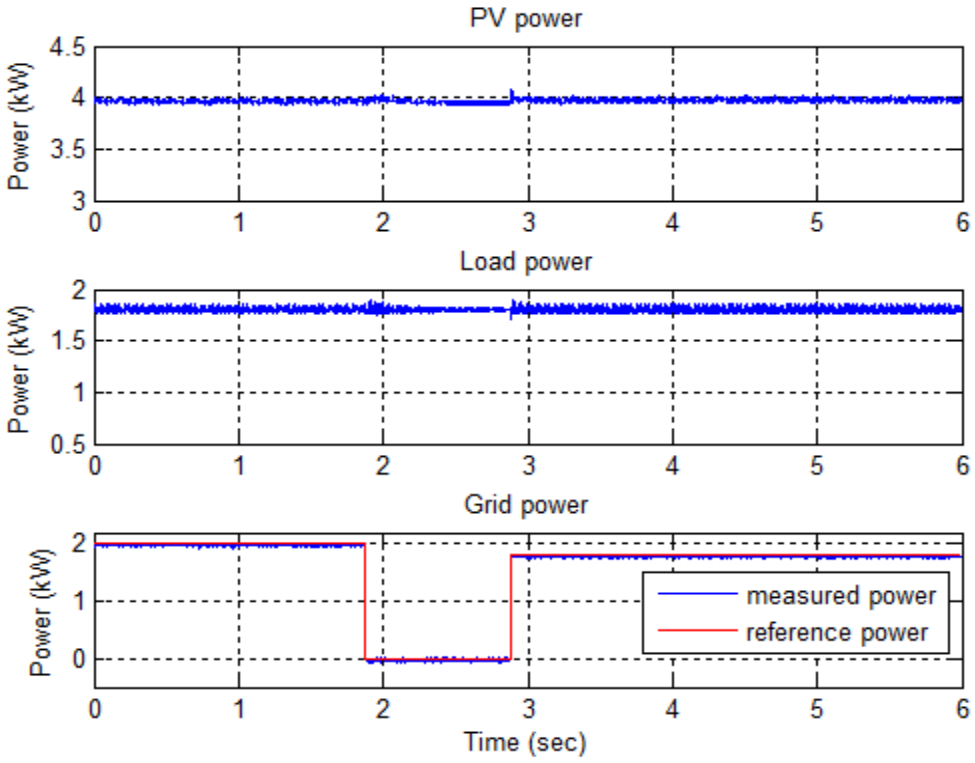

(a) Variation in PV power, load power and grid power

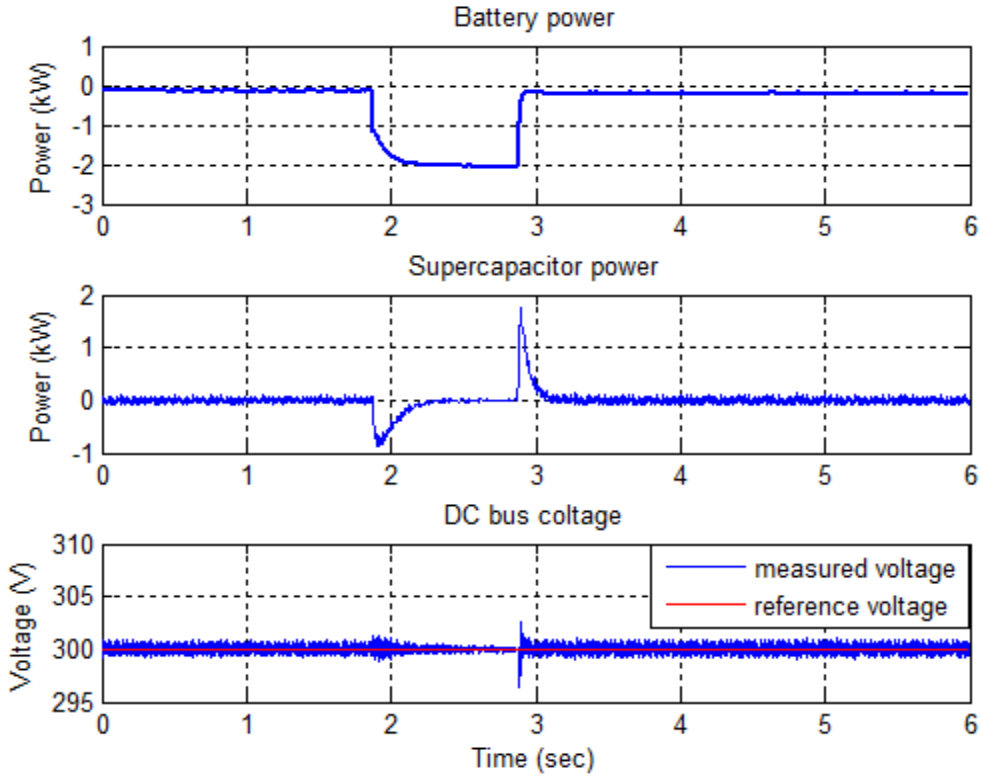

(b) Variation in battery power, supercapacitor power and DC bus voltage

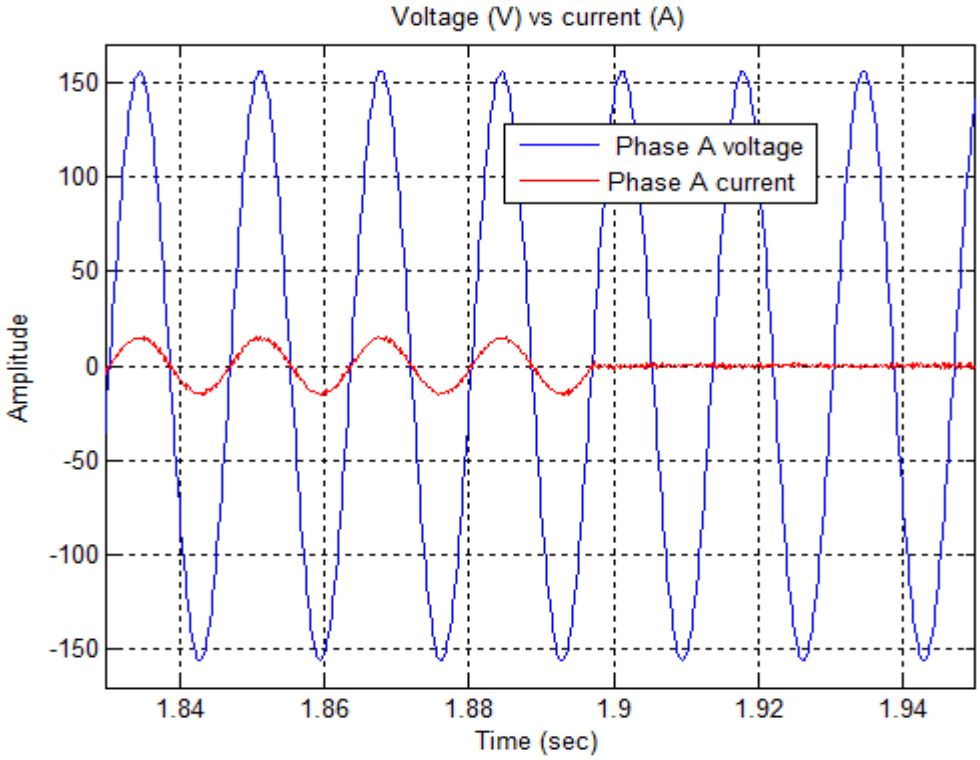

(c) Phase A voltage (phase to ground) and current variation

Figure 4.8 : Simulation of islanded mode

During islanding period, the rate of charge of battery increases and the transient caused by the mode switching is suppressed successfully by supercapacitor (P_{sc}) due its faster dynamic response. Phase A voltage and current of the main grid is shown in Figure 4.8 (c) which shows that current becomes zero at the instant of islanding. The fluctuation in the DC bus voltage caused by mode switching is shown in Figure 4.8 (b) which is negligible (less than 2%). Thus ESS successfully handles mode transition by regulating the DC bus voltage.

Performance of MPC to regulate the power exchange through VSC is compared with PI controller. The grid power reference is varied from 2 kW to 1 kW as shown in Figure 4.9.

Both MPC and PI based VSC track the reference power with zero steady state error. However, PI controller exhibits overshoot during transient as well as larger settling time than MPC. On the other hand, MPC tracks the reference with faster dynamic response and zero overshoot.

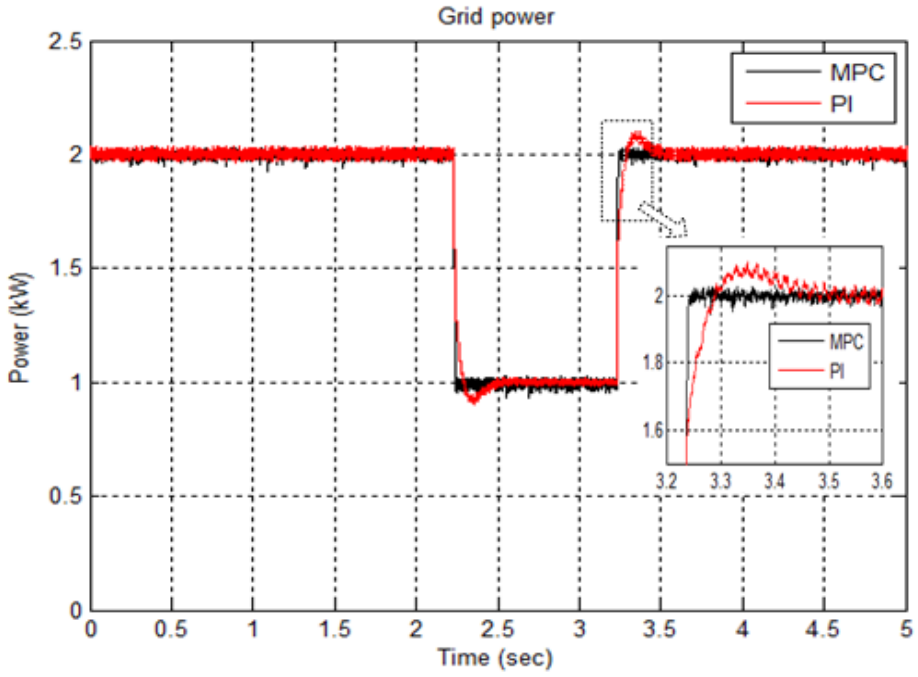

Figure 4.9 : Grid power with MPC and PI controlled VSC

4.4.3 Grid Connected Mode (Night)

During night, the sunlight disappears causing zero PV power production and as the worst case it is assumed that the capacity of ESS has been reduced to the level that is not sufficient to meet the local load. The microgrid works in the grid connected mode and DC bus voltage is controlled by grid converter. The load is supplied by the utility grid which acts as a rectifier in this case and ESS remains in the floating mode. As shown in Figure 4.10 (a), PV power production becomes completely zero at the instant of 1.2 second increasing the power transfer from main grid from 1.57 kW to 1.8 kW to meet the microgrid load.

The performance of the MPC based VSC to control DC bus voltage is compared against PI controlled VSC as shown in Figure 4.10 (c).

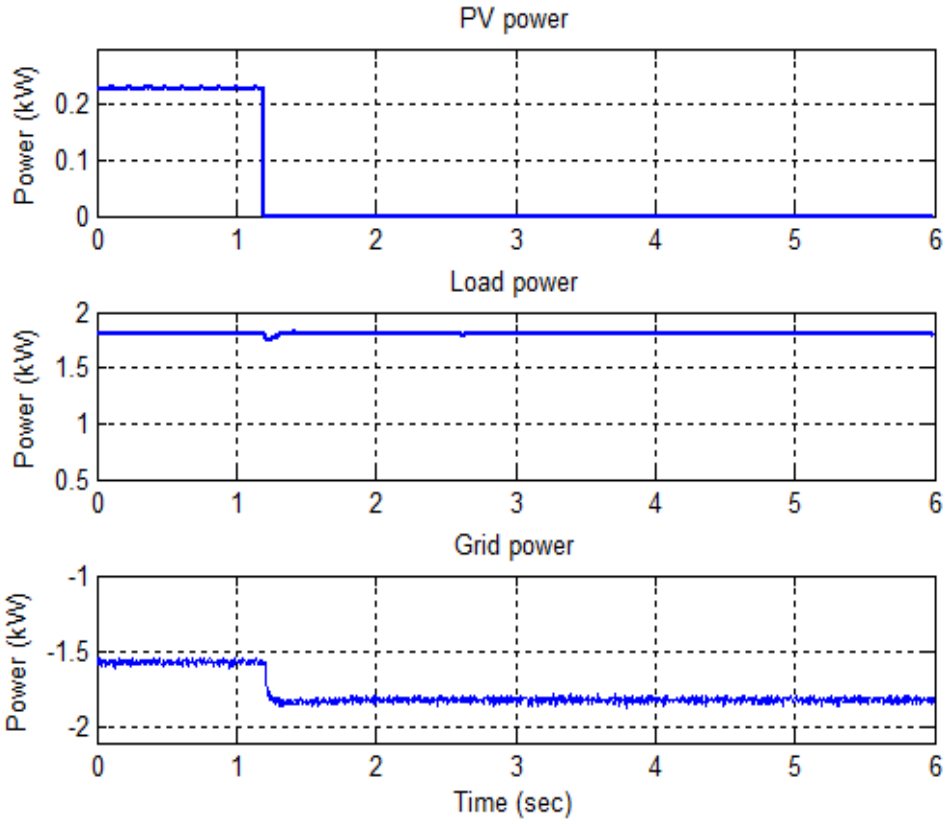

(a) Variation in PV power, load power and grid power

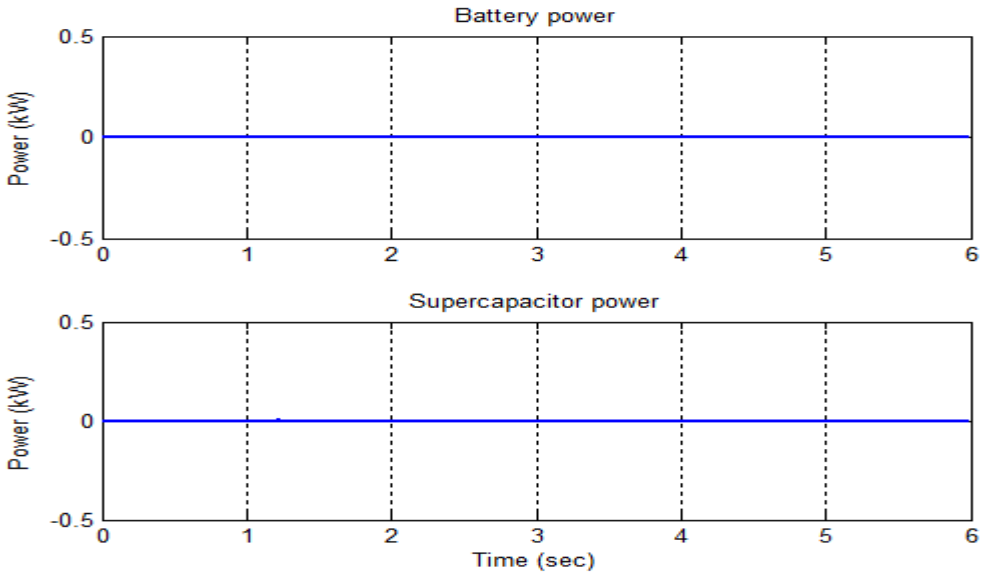

(b) Battery and supercapacitor power

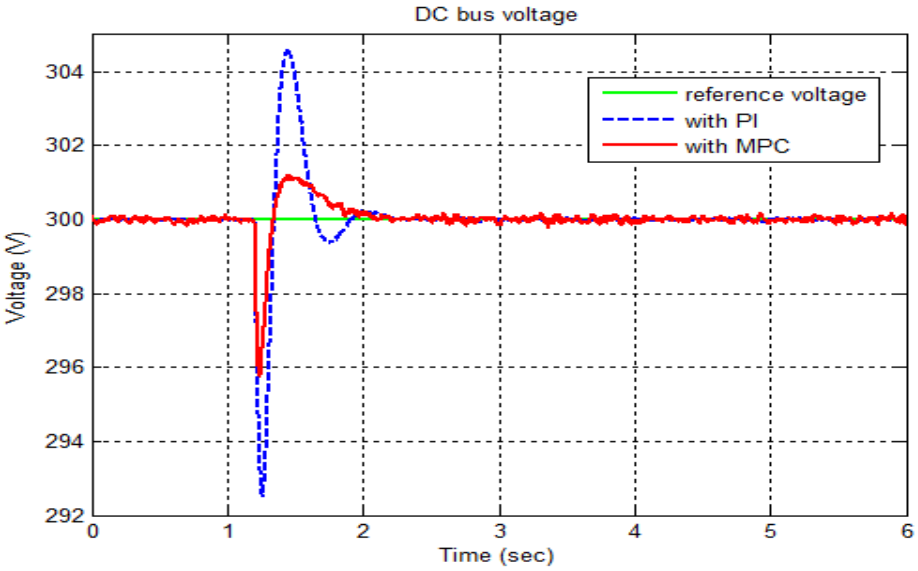

(c) DC Bus Voltage with MPC based VSC

Figure 4.10 : Simulation of grid connected mode (Night)

It is seen that in regulating DC bus voltage PI controlled VSC exhibits larger overshoot and settling time compared to the MPC based VSC. Due to the faster dynamic response MPC based VSC controller regulates the bus voltage with little fluctuation caused by fall of PV power.

In addition to meeting the load power, the main grid supplies battery charging power. Simulation of the battery charging process is shown in Figure 4.11. For battery charging, widely used constant current constant voltage (CC-CV) method has been adopted. In CC-CV charging, at first battery is charged with constant current (CC) and then switch to constant voltage (CV) mode when battery voltage reaches to its upper threshold. The battery is charged for 15 minutes with an initial state of charge (SoC) of 70 percent. After 7.5 minutes (450 seconds) of charging at constant current (12A) when battery voltage touches its upper limit (125V), the rest of the charging is done in CV mode. The charging current is assumed positive.

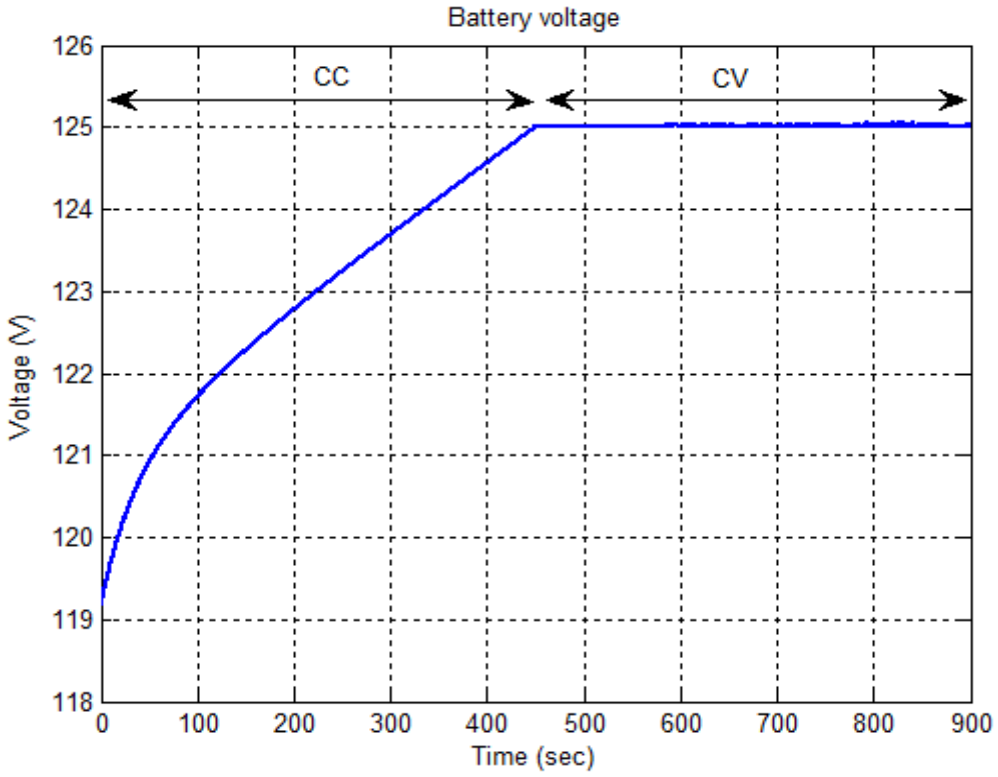

(a) Battery Voltage

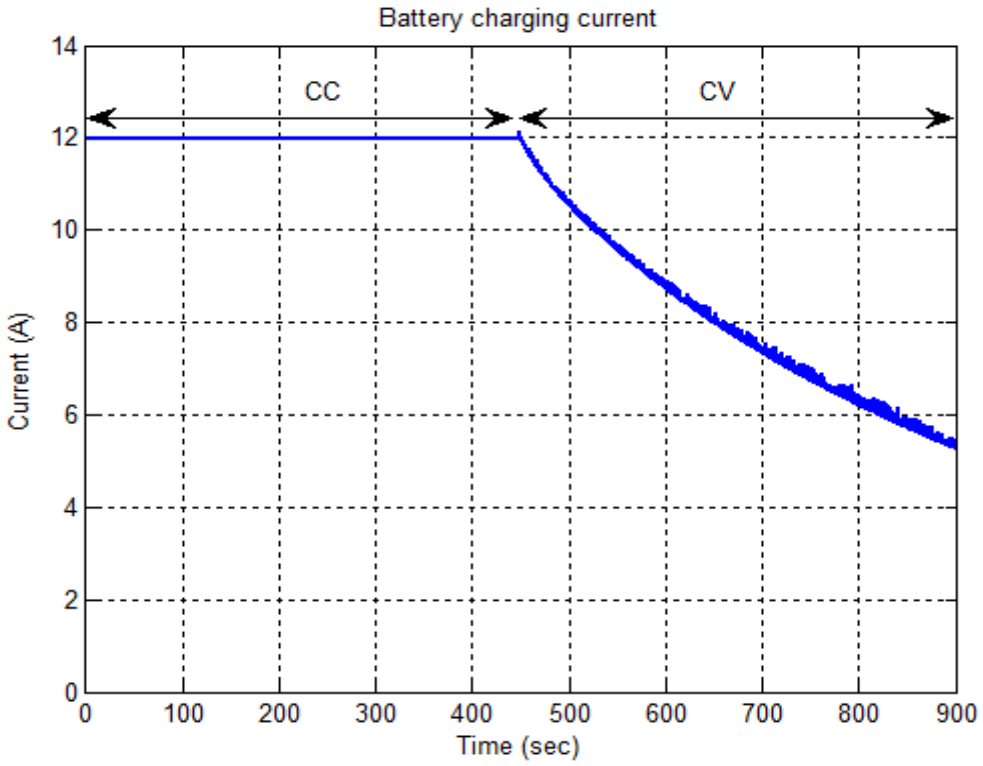

(b) Battery charging current

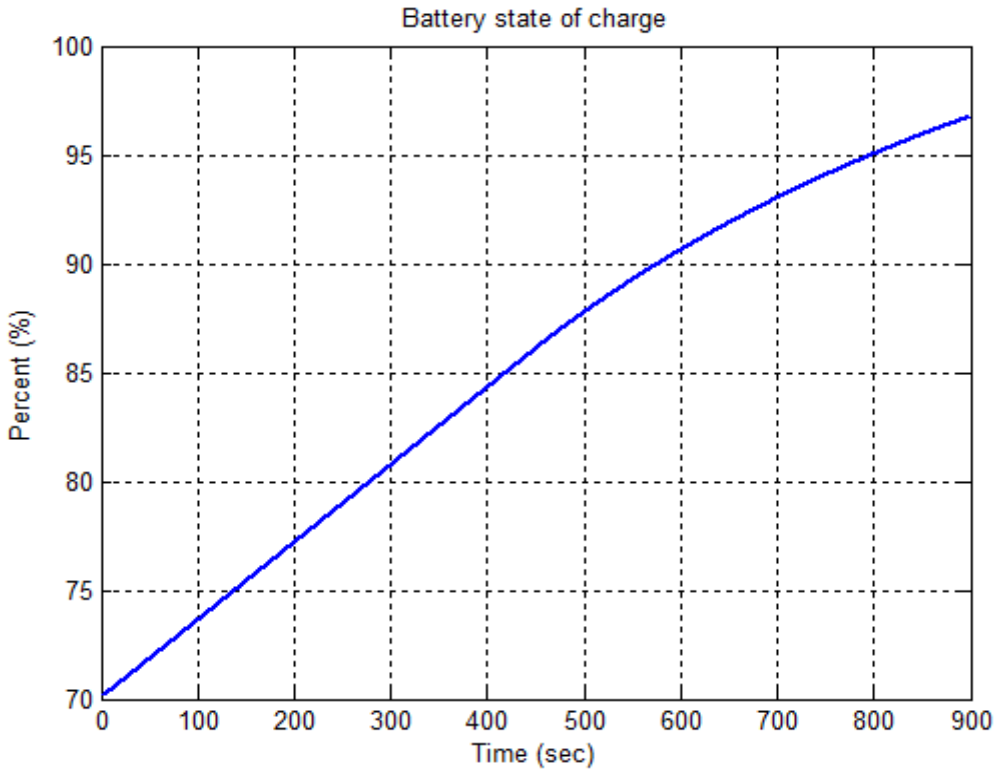

(c) Battery state of charge

Figure 4.11 : Simulation of battery charging in grid connected mode (Night)

4.5 Real Time Hardware in the Loop Experiment

In order to verify the effectiveness of the proposed control strategy experimental work is performed using real time hardware in the loop (RTHIL) setup. The arrangement for the RTHIL experiment is shown in Figure 4.12.

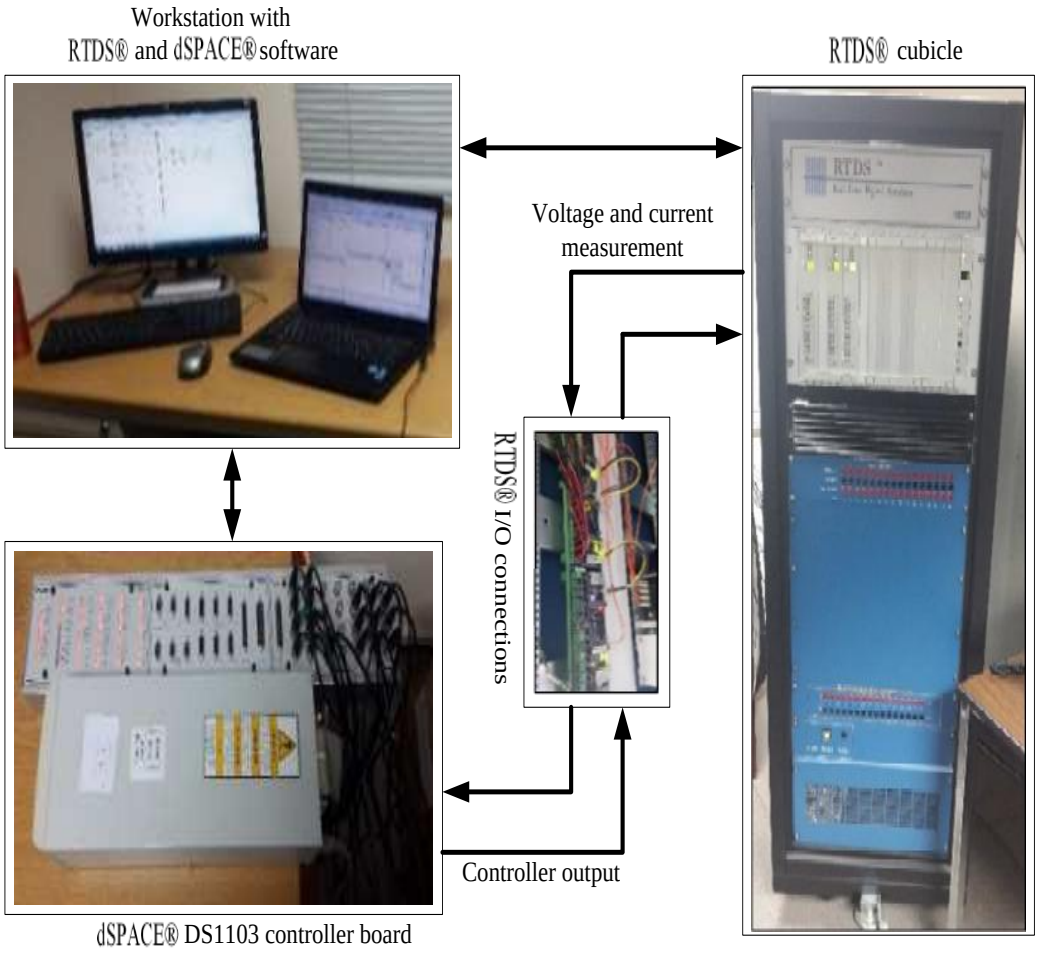

Figure 4.12 : Real time hardware in the loop arrangement

The proposed converter controllers are developed on dSPACE DS1103 controller board while the RTDS is used for simulation of plant model for microgrid. The RTDS and dSPACE exchange signals by their I/O connections. The controllers are implemented using the blocks of dSPACE tool box and SIMULINK. The dSPACE toolbox "rti1103" is integrated with

SIMULINK which contains the blocks for receiving and sending signal from DS1103 board. After the controller is implemented, it is downloaded to the processor of board using "Build Model" command and then the controller is ready to use for experimental work. The schematic of the system in RSCAD and controller in dSPACE are shown in Figure 4.13 and Figure 4.14 respectively.

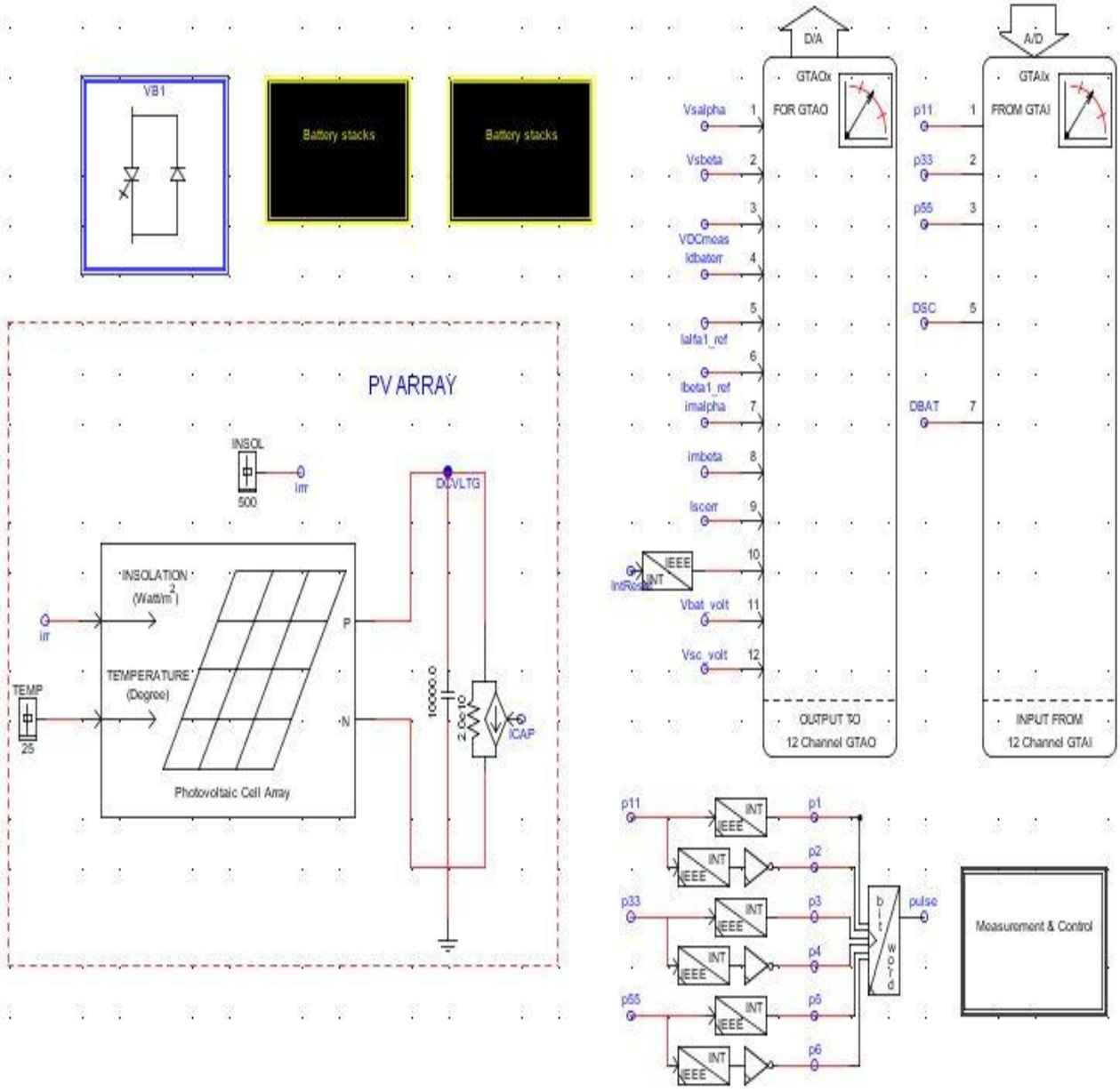

Figure 4.13 : System model in RSCAD for RTHIL experiment

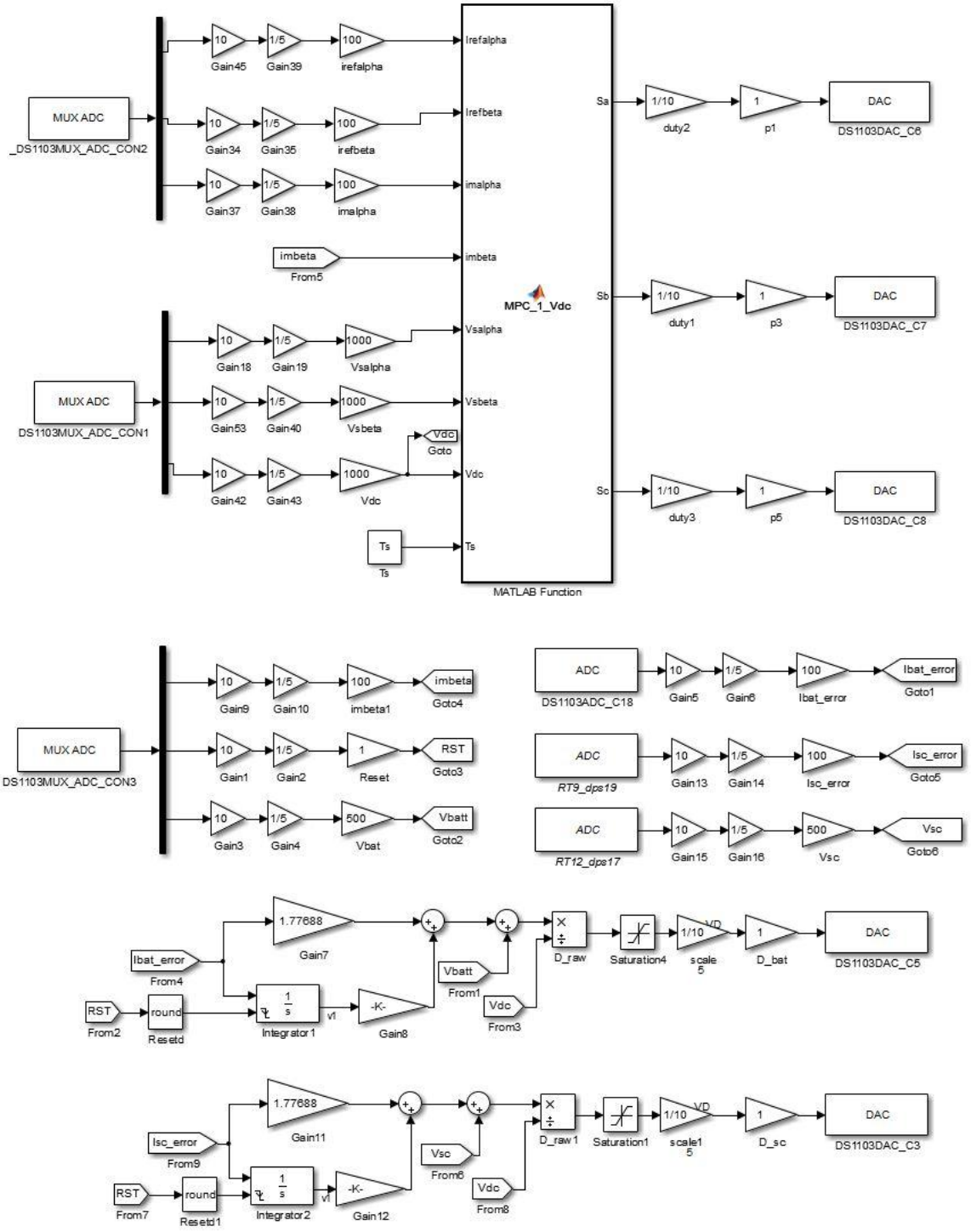

Figure 4.14: Schematic of Controllers implemented in dSPACE

4.6 Experimental Results

All of the three simulation cases, case I: grid connected mode (day), case II: islanded mode, and case III: grid connected mode (night) are considered for experiment and obtained results are compared with that of the simulations.

Case I: Grid connected mode (day)

Same variations in the PV power and grid power demand as in the simulation are applied for experimental study. The resulting variations in the dc bus voltage, grid power, load power, and energy storage power are presented and compared with simulation results in Figure 4.15. Experimental results resemble the simulation results with negligible deviation which demonstrates satisfactory performance the proposed controllers.

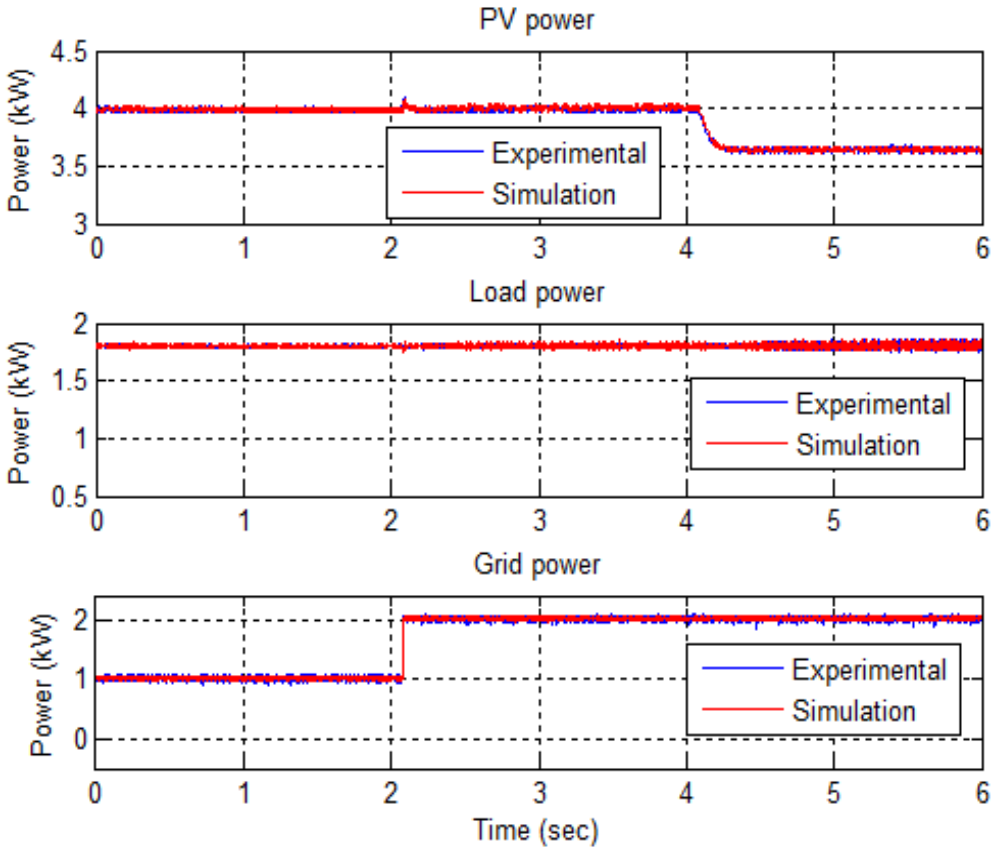

(a) Variation in PV power, load power and grid power

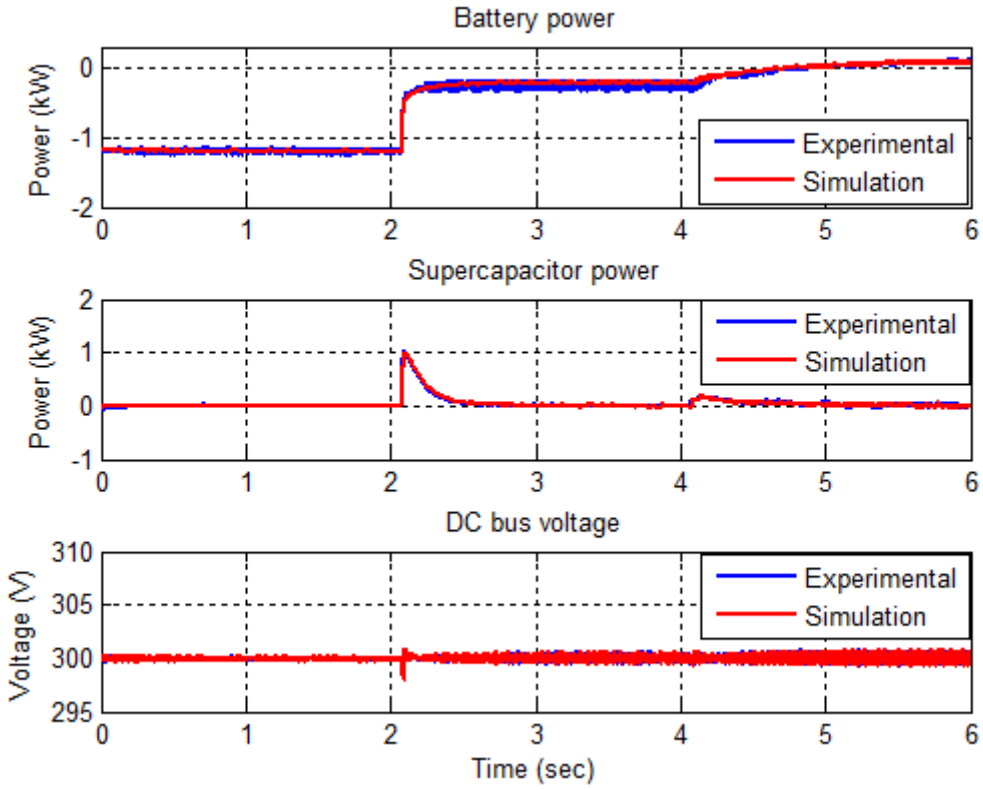

(b) Variation in battery power, supercapacitor power and DC bus voltage

Figure 4.15 : Experimental results of grid connected mode (day)

Case II: Islanded mode

In this case microgrid is islanded for 1 second and then reconnected to the grid again. The purpose of this experiment is to check the performance of the proposed controllers for smooth mode transition without affecting system stability. As seen from Figure 4.16, the transients caused by mode switching are suppressed by energy storage system and faster response of VSC controller. A good similarity between simulation and experimental results are achieved.

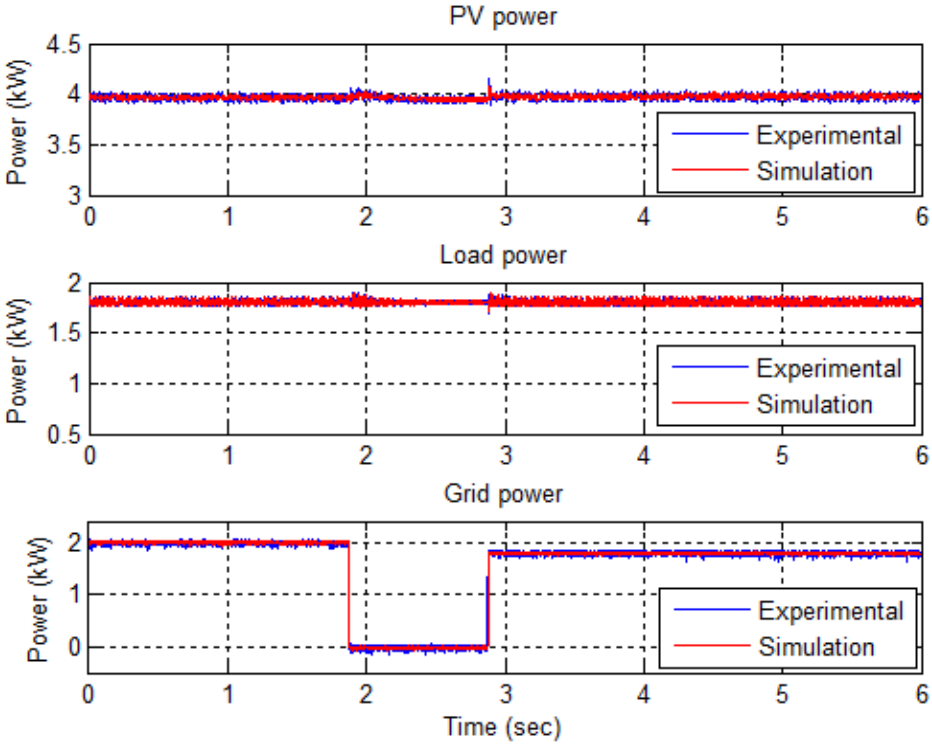

(a) Variation in PV power, load power and grid power

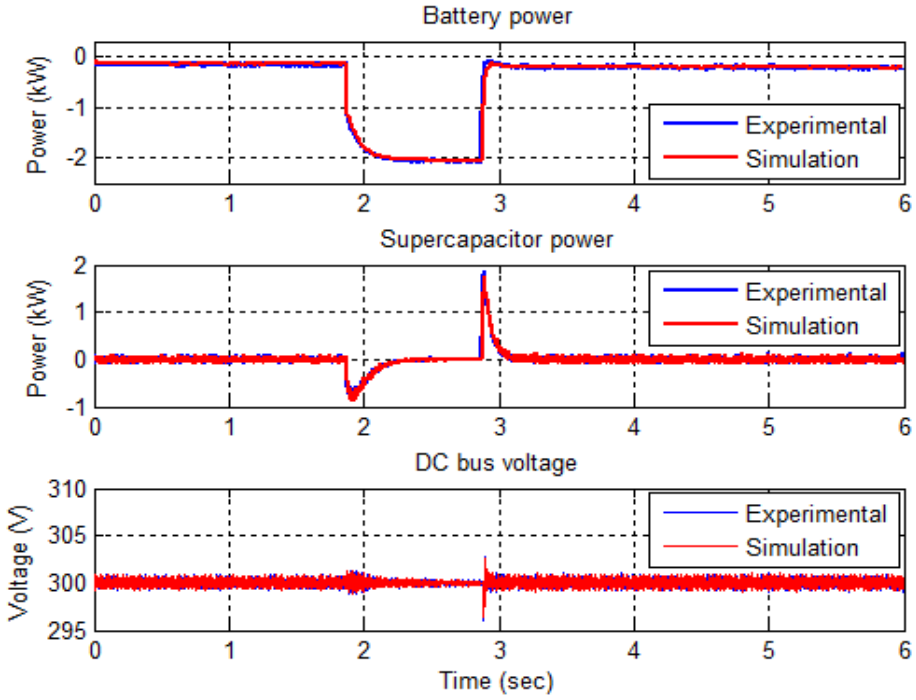

(b) Variation in battery power, supercapacitor power and DC bus voltage

Figure 4.16 : Experimental results of islanded mode

Case III: Grid connected mode (night)

Similar to the simulation study, PV power is set to zero in this test and performance of VSC controller is tested. As shown in Figure 4.17 (c), although higher oscillations are observed in the DC bus voltage than the simulation result it tracks the reference value well. Variation in the grid power is shown in Figure 4.17 (a) which also follows the simulation result.

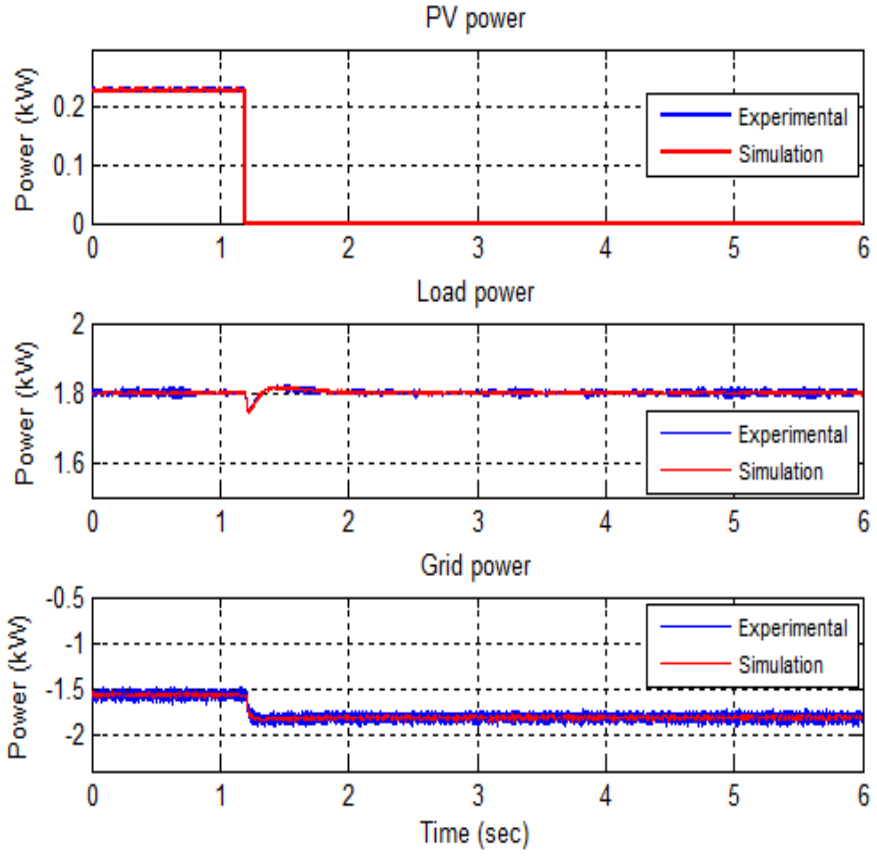

(a) Variation in PV power, load power and grid power

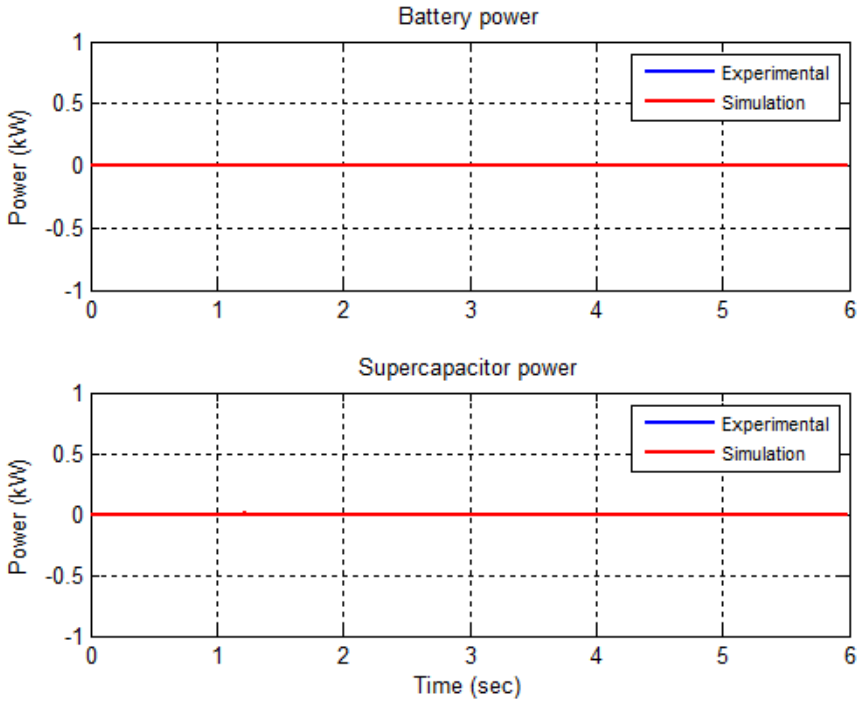

(b) Battery power and supercapacitor power

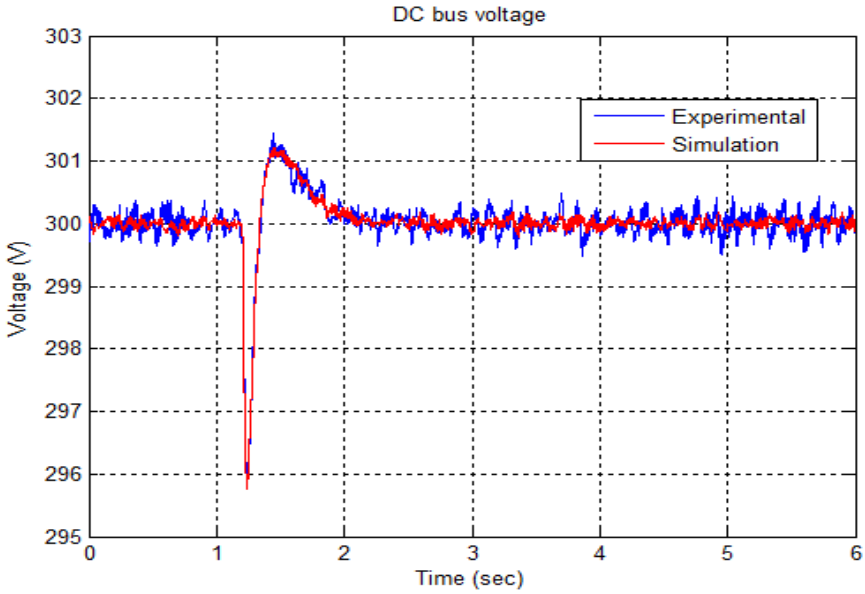

(c) DC bus voltage variation

Figure 4.17 : Experimental results of grid connected mode (night)

The performance of the controllers is seen to be robust to maintain current and voltage regulation even in case of transients caused by PV power and grid power variations.

4.7 Performance Comparison of the Proposed Controller to Existing Methods in Literature

In the grid connected mode, dc link voltage is controlled by energy storage system and power exchange with grid is controlled by VSC controller. The transient performance of the DC link voltage controller and VSC controller of reference [57] is compared with proposed control system.

In reference [57], the power exchange through VSC is controlled by direct power control (DPC) based controller and DC link voltage is regulated by PI based bidirectional buck-boost converter controller. From Figure 4.18 it is seen that proposed MPC based VSC controller follows the reference grid power without any overshoot during transients. However, overshoots in the grid power are observed during each transition of grid power reference with DPC based controller presented in [57]. This proves the superiority of proposed MPC based controller.

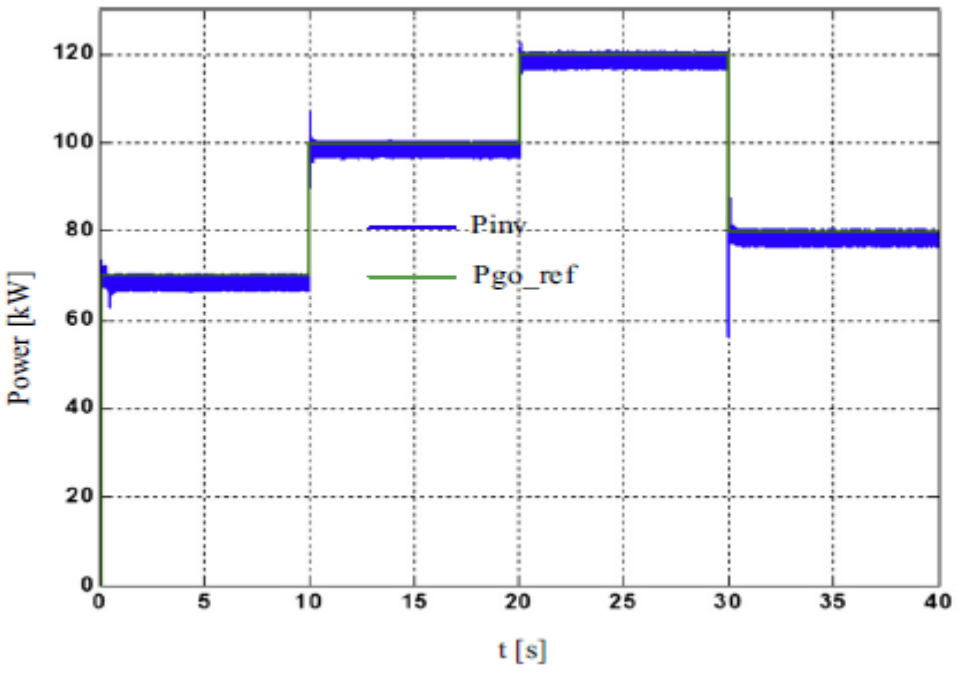

(a) Tracking of grid power in reference [57]

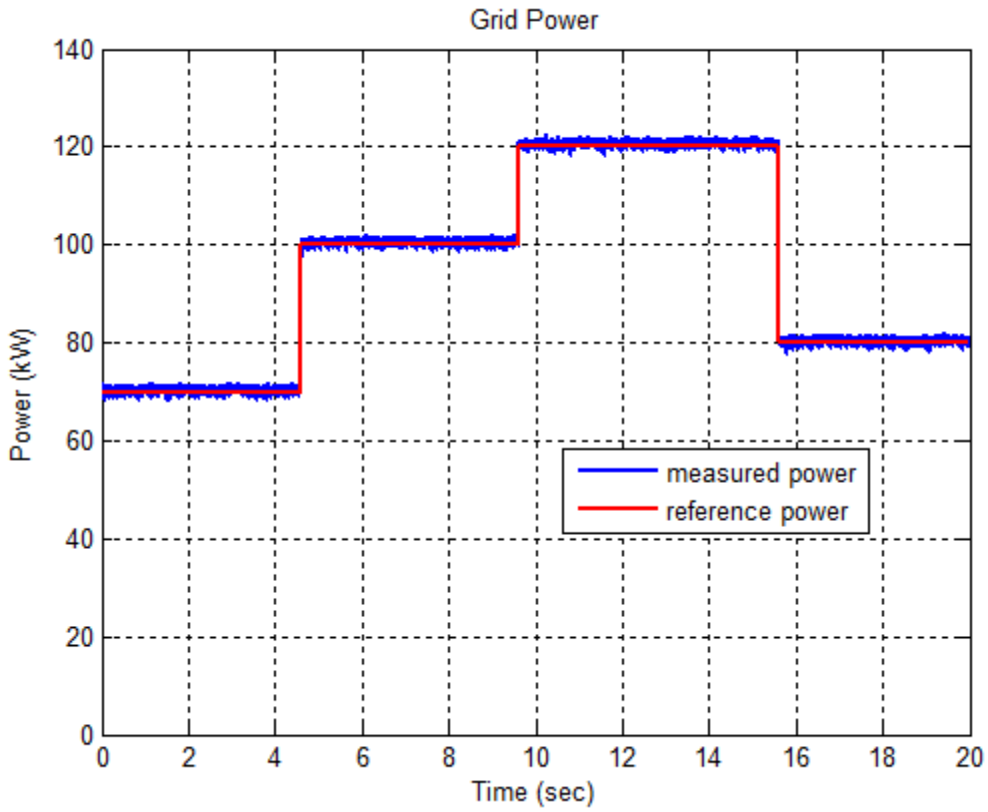

(b) Tracking of grid power reference with proposed MPC

Figure 4.18 : Performance comparison of current controller

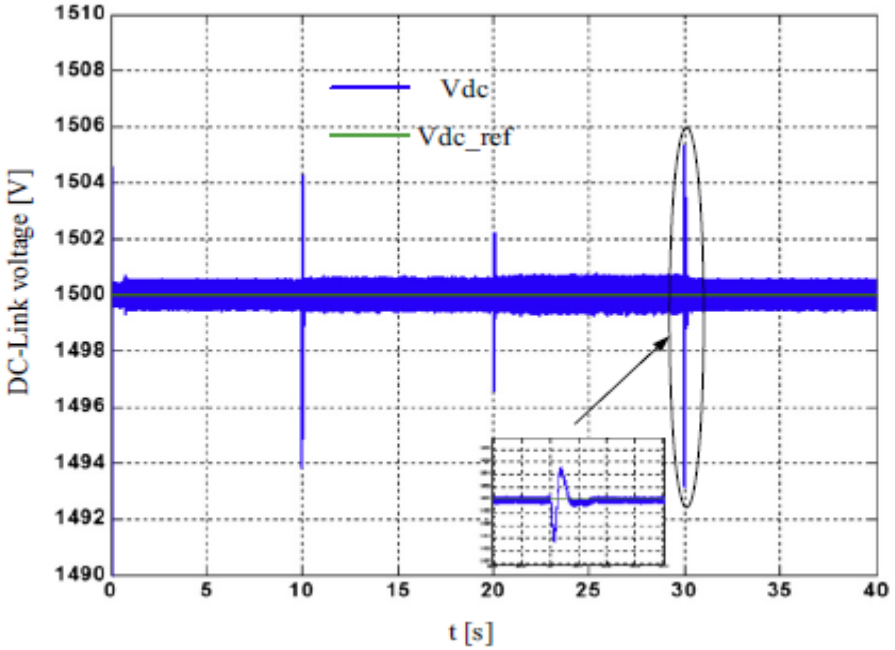

(a) DC link voltage variation in reference [57]

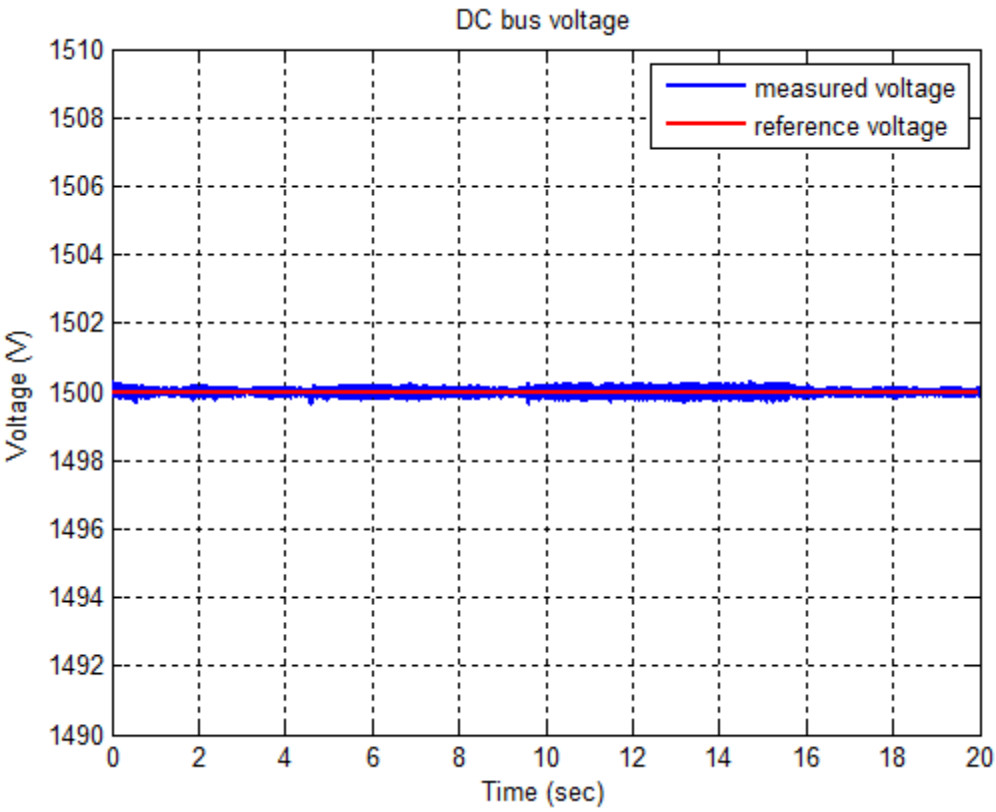

(b) DC link voltage with proposed control

Figure 4.19 : Performance comparison of voltage regulation

The performance of the energy storage converter controller for voltage regulation is presented in Figure 4.19. It is clear from the DC bus voltage waveshapes that both proposed controller and controller of reference [57] perform well to regulate the bus voltage with little variation.

CHAPTER 5

CONCLUSIONS AND FUTURE WORK

5.1 Conclusions

DC microgrid has the potential for improving power system stability, reliability and efficiency. In this work, low voltage small scale DC microgrid with PV source and hybrid energy storage system is developed.

Different control strategies for controlling DC microgrid are discussed. Among them decentralized control strategy without requiring any communication technology is proposed for the energy management in the microgrid. DC bus voltage is used for coordination among different modules of microgrid to maintain power balance during both grid connected and islanded modes of microgrid. This increases reliability by avoiding the use of communication links.

Model predictive control of voltage source converter is proposed for regulating the power exchange between microgrid and utility grid. Frequency approach of power sharing is used to divide the low frequency and high frequency component of power between battery and supercapacitor respectively.

Both grid connected and islanded modes of the microgrid are studied considering the variations in the PV power and grid power demand. Transients caused by the power variations in the microgrid are successfully suppressed by the proposed energy storage control system with little variation in the DC bus voltage. Proposed model predictive controller outperforms classical PI controller in regulating power exchange between microgrid and utility grid.

The proposed control strategies and system models are developed using RSCAD software and simulated in the real time environment using RTDS. The simulation results verify the effectiveness of the proposed control systems. Further, real time hardware in the loop (RTHIL) experimental results using RTDS and dSPACE demonstrate the suitability of the proposed control techniques for implementation in practical system.

5.2 Future Work

The suggestions for the future work are given below

- During islanded mode, if load power is greater than PV plus storage capacity the microgrid will be unstable. Automatic load shedding scheme can be developed in order to overcome this problem.
- Islanding detection algorithms on AC microgrid are based on phase and frequency. Due the absence of phase and frequency those algorithms can not be applied in DC system. New methods for islanding detection for DC system can be developed.
- Two modes of operation of microgrid complicate the design of protection schemes. Universal protection system for both modes can be studied and implemented.
- Fault ride through capability of the microgrid can be studied.

References

[1] B.T. Patterson, "DC, come home: DC microgrids and the birth of the Enernet," *IEEE Power Energy Magazine, 10*, pp. 60–69, 2012.

[2] D. Z. G.C. Lazaroiu, "Improvements, A control system for dc arc furnaces for power quality," *Electr. Power Syst. Res.*, vol. 80, no. 12, pp. 1498–1505, 2010.

[3] Ahmed T. Elsayed, Ahmed A. Mohamed, and Osama A. Mohamed,, "DC microgrids and distribution systems: an overview," *Electr. Power Syst. Res.*, vol. 119, pp. 407–417, 2015.

[4] D. Chen and L. Xu, "Autonomous DC voltage control of a DC microgrid with multiple slack terminals," *IEEE Trans. Power Syst.*, vol. 27, no. 4, pp. 1897–1905, 2012.

[5] Z. W. Q. Zhong, L. Lin, and Y. Zhang, "Study on the Control Strategies and Dynamic Performance of DC Distribution Network," in *IEEE Power and Energy Society General Meeting*, pp. 1–5, 2012.

[6] C. N. Papadimitriou, E. I. Zountouridou, and N. D. Hatziargyriou, "Review of hierarchical control in DC microgrids," *Electr. Power Syst. Res.*, vol. 122, pp. 159–167, 2015.

[7] Zhihong Ye, D. Boroyevich, Kun Xing, F.C. Lee, "Design of parallel sources in DC distributed power systems by using gain-scheduling technique," in *IEEE Annual Power Electronics Specialists Conference*, pp. 161–165, 1999.

[8] Z. H. Jian, Z. Y. He, J. Jia, and Y. Xie, "A review of control strategies for DC micro-grid," *Proc. Int. Conf. Intell. Control Inf. Process. ICICIP 2013*, pp. 666–671, 2013.

[9] N. Hatziargyriou, *Microgrids: Architectures and Control*. Wiley, IEEE Press,Athens, 2014.

[10] M. G. S. Anand, B.G. Fernandes, "Distributed control to ensure pro-portional load sharing and improve voltage regulation in low voltage DC microgrids," *IEEE Trans. Power Electron.*, vol. 28, no. 4, pp. 1900 – 1913, 2013.

[11] H. Kakigano, Y. Miura, and T. Ise, "Distribution voltage control for DC microgrids using fuzzy control and gain-scheduling technique," *IEEE Trans. Power Electron.*, vol. 28, no. 5, pp. 2246–2258, 2013.

[12] P. Dong, D.; Cvetkovic, I.; Boroyevich, D.; Zhang, W.; Wang, R.; Mattavelli, "Grid-interface bi-directional converter for residential DC distribution systems—-Part one:

High-density two-stage topology," *IEEE Trans. Power Electron.*, vol. 28, no. 4, pp. 1655 – 1666, 2013.

[13] T. Dragicevic, J. M. Guerrero, J. C. Vasquez, and D. Skrlec, "Supervisory control of an adaptive-droop regulated DC microgrid with battery management capability," *IEEE Trans. Power Electron.*, vol. 29, no. 2, pp. 695–706, 2014.

[14] X. Lu, J. M. Guerrero, and K. Sun, "An Improved Droop Control Method for DC Microgrids Based on Low Bandwidth Communication With DC Bus Voltage Restoration and Enhanced Current Sharing Accuracy," *IEEE Trans. Power Electron.*, vol. 29, no. 4, pp. 1800–1812, 2014.

[15] R. Asad and A. Kazemi, "A novel decentralized voltage control method for direct current microgrids with sensitive loads," *Int. Trans. Electr. Energy Syst.*, 2013.

[16] L. H. and J. U. J.M. Guerrero, "Control of Distributed Uninterruptible Power Supply Systems," *IEEE Trans. Ind. Electron.*, vol. 55, no. 8, pp. 2845 – 2859, 2008.

[17] X. Lu, J. M. Guerrero, K. Sun, and J. C. Vasquez, "An improved droop control method for dc microgrids based on low bandwidth communication with dc bus voltage restoration and enhanced current sharing accuracy," *IEEE Trans. Power Electron.*, vol. 29, no. 4, pp. 1800–1812, 2014.

[18] R. L. H. Xiaonan Lu; Guerrero, J.M.; Kai Sun; Vasquez, J.C.; Teodorescu, "Hierarchical control of parallel AC–DC converter interfaces for hybrid microgrids," *IEEE Trans. Smart Grid*, vol. 5, no. 2, pp. 683–692, 2014.

[19] T. Dragičević, J. M. Guerrero, and J. C. Vasquez, "A distributed control strategy for coordination of an autonomous LVDC microgrid based on power-line signaling," *IEEE Trans. Ind. Electron.*, vol. 61, no. 7, pp. 3313–3326, 2014.

[20] X. Lu, K. Sun, J. M. Guerrero, J. C. Vasquez, and L. Huang, "State-of-Charge Balance Using Adaptive Droop Control for Distributed Energy Storage Systems in DC Microgrid Applications," *IEEE Trans. Ind. Electron.*, vol. 61, no. 6, pp. 2804–2815, 2014.

[21] X. Lu, K. Sun, J. M. Guerrero, J. C. Vasquez, and L. Huang, "Double-Quadrant State-of-Charge Based Droop Control Method for Distributed Energy Storage Systems in Autonomous DC Microgrids," *IEEE Trans. Smart Grid*, vol. 6, no. 1, pp. 147 – 157, 2015.

[22] D. Wu, F. Tang, T. Dragicevic, J. M. Guerrero, and J. C. Vasquez, "Coordinated Control Based on Bus-Signaling and Virtual Inertia for DC Islanded Microgrids," *IEEE Trans. Smart Grid*, vol. 6, no. 6, pp. 1–12, 2015.

[23] P.-I. Hwang, G. Jang, G.-C. Pyo, B.-M. Han, S.-I. Moon, and S.-J. Ahn, "DC Microgrid

Operational Method for Enhanced Service Reliability Using DC Bus Signaling," *J. Electr. Eng. Technol.*, vol. 10, no. 2, pp. 452–464, 2015.

[24] P. Wang, C. Jin, D. Zhu, Y. Tang, P. C. Loh, and F. H. Choo, "Distributed Control for Autonomous Operation of a Three-Port AC/DC/DS Hybrid Microgrid," *IEEE Trans. Ind. Electron.*, vol. 62, no. 2, pp. 1279–1290, 2015.

[25] C. Jin, P. Wang, J. Xiao, Y. Tang, and F. H. Choo, "Implementation of hierarchical control in DC microgrids," *IEEE Trans. Ind. Electron.*, vol. 61, no. 8, pp. 4032–4042, 2014.

[26] B. D. P. Thounthong, S. Sikkabut, A. Luksanasakul, P. Koseeyaporn, P. Sethakul, and S. Pierfederici, "Fuzzy Logic Based DC Bus Voltage Control of a Stand Alone Photovoltaic/Fuel Cell/Supercapacitor Power Plant," in *11th International Conference on Environment and Electrical Engineering*, pp. 725 – 730, 2012

[27] X. R. Huang Jiayi, , Jiang Chuanwen, "A review on distributed energy resources and MicroGrid," *Renew. Sustain. Energy Rev.*, vol. 12, no. 9, pp. 2472–2483, 2008.

[28] R. Kim, H. R. Seo, G. H. Kim, M. Park, I. K. Yu, Y. Otsuki, J. Tamura, S. H. Kim, K. Sim, and K. C. Seong, "Operating characteristic analysis of HTS SMES for frequency stabilization of dispersed power generation system," *IEEE Trans. Appl. Supercond.*, vol. 20, no. 3, pp. 1334–1338, 2010.

[29] N. Eghtedarpour and E. Farjah, "Distributed charge/discharge control of energy storages in a renewable-energy-based DC micro-grid," *Renew. Power Gener. IET*, vol. 8, no. 1, pp. 45–57, 2014.

[30] X. Dou, X. Quan, Z. Wu, M. Hu, J. Sun, K. Yang, and M. Xu, "Improved Control Strategy for Microgrid Ultracapacitor Energy Storage Systems," *Energies*, vol. 7, no. 12, pp. 8095–8115, 2014.

[31] J.-D. Park, "Simple Flywheel EnergyStorage using Squirrel-cage Induction Machine for DC Bus Microgrid ni ",smetsyS*IEEE Industrial Electronics Society Conference*, pp. 3040–3045, 2010.

[32] T. Karaipoom and I.Ngamroo, "Enhancement of LVRT Performance and Alleviation of Power Fluctuation of DFIG Wind Turbine in DC Microgrid by ni ",SEMS*IEEE International Conference on Applied Superconductivity and Electromagnetic Devices*, , pp. 207–208, 2013.

[33] W. L. J. Li, and X. Zhang, "An Efficient Wind-Photovoltaic Hybrid Generation System For Dc Micro-Grid," in *IET 8th International Conference on Advances in Power System Control, Operation and Management*, pp. 1–6, 2009.

[34] F. Ferret and M. Simões, *Integration of Alternative Sources of Energy: Storage Systems*. Wiley-IEEE Press, 2006.

[35] J. Stevens and B. Schenkman, "DC Energy Storage in the CERTS Microgrid." Sandia National Laboratories, 2008.

[36] L. Xu and D. Chen, "Control and operation of a DC microgrid with variable generation and energy storage," *IEEE Trans. Power Deliv.*, vol. 26, no. 4, pp. 2513–2522, 2011.

[37] T. Ma, B. Serrano, and O. Mohammed, "Distributed control of hybrid AC-DC microgrid with solar energy, energy storage and critical load," *in Clemson Univ. Power Syst. Conf.*, pp. 1–6, 2014.

[38] F. F. and M. Simões, *Integration of Alternative Sources of Energy: Storage Systems*. Wiley-IEEE Press, 2006.

[39] W. .J .LLi, and X.gnahZ, "An EfficientWind-Photovoltaic Hybrid Generation System For Dc Micro-Grid," in *IET 8th International Conference on Advances in Power System Control, Operation and Management*, , pp. 1–6, 2009.

[40] H. Kakigano, Y. Miura, and T. Ise, "Low-Voltage Bipolar-Type DC Microgrid for Super High Quality Distribution," *IEEE Trans. Power Electron.*, vol. 25, no. 12, pp. 3066–3075, Dec. 2010.

[41] Y. Zhang and Y. W. Li, "Energy Management Strategy for Supercapacitor in Droop-controlled DC Microgrid Using Virtual Impedance," *IEEE Trans. Power Electron.*, pp. 1–1, 2016.

[42] X. Chang, Y. Li, W. Zhang, N. Wang, and W. Xue, "Active Disturbance Rejection Control for a Flywheel Energy Storage System," *IEEE Trans. Ind. Electron.*, vol. 62, no. 2, pp. 991–1001, Feb. 2015.

[43] L. Chen, H. He, L. Zhu, F. Guo, Z. Shu, X. Shu, and J. Yang, "Coordinated Control of SFCL and SMES for Transient Performance Improvement of Microgrid With Multiple DG Units," *Can. J. Electr. Comput. Eng.*, vol. 39, no. 2, pp. 158–167, 2016.

[44] H. Zhou, T. Bhattacharya, D. Tran, T. S. T. Siew, and A. M. Khambadkone, "Composite Energy Storage System Involving Battery and Ultracapacitor With Dynamic Energy Management in Microgrid Applications," *IEEE Trans. Power Electron.*, vol. 26, no. 3, pp. 923–930, 2011.

[45] A. Tani, M. B. Camara, and B. Dakyo, "Energy management in the decentralized generation systems based on renewable energy sources," *2012 Int. Conf. Renew. Energy Res. Appl.*, vol. 51, no. 1, pp. 1–6, 2012.

[46] T. Christen and M. W. Carlen, “Theory of Ragone plots,” *J. Power Sources*, vol. 91, no. 2, pp. 210–216, 2000.

[47] S. Liu and R. A. Dougal, “Dynamic Multiphysics Model for Solar Array,” *Int. Trans. Energy Convers.*, vol. 17, no. 2, pp. 285–294, 2002.

[48] E. R. F. M. G. Villalva, and J. R. Gazoli, “Comprehensive Approach to Modeling and Simulation of Photovoltaic Arrays,” *IEEE Trans. Power Electron.*, vol. 24, no. 5, pp. 1198 – 1208, 2009.

[49] M. G. Villalva, T. G. de Siqueira, and E. Ruppert, “Voltage regulation of photovoltaic arrays: small-signal analysis and control design,” *IET Power Electron.*, vol. 3, no. 6, p. 869, 2010.

[50] Kaiyuan Li and King Jet Tseng, “Energy efficiency of lithium-ion battery used as energy storage devices in micro-grid,” *Applied Power Electronics Conference and Exposition (APEC)*. pp. 3422–3430, 2016.

[51] Z. M. Salameh, M. A. Casacca, and W. A. Lynch, “A mathematical model for lead-acid batteries,” *IEEE Trans. Energy Convers.*, vol. 7, no. 1, pp. 93–98, Mar. 1992.

[52] S. Buller, M. Thele, R. W. A. A. DeDoncker, and E. Karden, “Impedance-Based Simulation Models of Supercapacitors and Li-Ion Batteries for Power Electronic Applications,” *IEEE Trans. Ind. Appl.*, vol. 41, no. 3, pp. 742–747, May 2005.

[53] L. Benini, G. Castelli, A. Macii, E. Macii, M. Poncino, and R. Scarsi, “Discrete-time battery models for system-level low-power design,” *IEEE Trans. Very Large Scale Integr. Syst.*, vol. 9, no. 5, pp. 630–640, Oct. 2001.

[54] C. Min and G. A. Rincon-Mora, “Accurate electrical battery model capable of predicting runtime and I-V performance,” *IEEE Trans. Energy Convers.*, vol. 21, no. 2, pp. 504–511, 2006.

[55] N. Mohan, T. M. Undeland, and W. P. Robbins, *Power electronics : converters, applications, and design*. John Wiley & Sons, 2003.

[56] J. A. Suul, K. Ljokelsoy, T. Midtsund, and T. Undeland, “Synchronous Reference Frame Hysteresis Current Control for Grid Converter Applications,” *IEEE Trans. Ind. Appl.*, vol. 47, no. 5, pp. 2183–2194, Sep. 2011.

[57] A. Choudar, D. Boukhetala, S. Barkat, and J.-M. Brucker, “A local energy management of a hybrid PV-storage based distributed generation for microgrids,” *Energy Convers. Manag.*, vol. 90, pp. 21–33, 2015.

[58] L. Xu, D. Zhi, and L. Yao, “Direct Power Control of Grid Connected Voltage Source

Converters," *2007 IEEE Power Engineering Society General Meeting*. IEEE, pp. 1–6, Jun-2007.

[59] B. Singh and N. K. Swami Naidu, "Direct Power Control of Single VSC-Based DFIG Without Rotor Position Sensor," *IEEE Trans. Ind. Appl.*, vol. 50, no. 6, pp. 4152–4163, Nov. 2014.

[60] A. Bouafia, F. Krim, and J.-P. Gaubert, "Fuzzy-Logic-Based Switching State Selection for Direct Power Control of Three-Phase PWM Rectifier," *IEEE Trans. Ind. Electron.*, vol. 56, no. 6, pp. 1984–1992, Jun. 2009.

[61] J. Hu, L. Shang, Y. He, and Z. Q. Zhu, "Direct Active and Reactive Power Regulation of Grid-Connected DC/AC Converters Using Sliding Mode Control Approach," *IEEE Trans. Power Electron.*, vol. 26, no. 1, pp. 210–222, Jan. 2011.

[62] M. Yazdanian and A. Mehrizi-Sani, "Internal model-based current control of the RL filter-based voltage-sourced converter," *IEEE Trans. Energy Convers.*, vol. 29, no. 4, pp. 873–881, Dec. 2014.

[63] P. C. Jose Rodriguez, *Predictive Control of Power Converters and Electrical Drives*. Wiley-IEEE Press, 2012.

[64] J. Rodriguez, M. P. Kazmierkowski, J. R. Espinoza, P. Zanchetta, H. Abu-Rub, H. A. Young, and C. A. Rojas, "State of the Art of Finite Control Set Model Predictive Control in Power Electronics," *IEEE Trans. Ind. Informatics*, vol. 9, no. 2, pp. 1003–1016, May 2013.

[65] P. Cortes, J. Rodriguez, C. Silva, and A. Flores, "Delay Compensation in Model Predictive Current Control of a Three-Phase Inverter," *IEEE Trans. Ind. Electron.*, vol. 59, no. 2, pp. 1323–1325, Feb. 2012.

[66] R. I. Amirnaser Yazdani, *Voltage-Sourced Converters in Power Systems : Modeling, Control, and Applications*. IEEE Press/John Wiley, 2010.

[67] S. Ahmad Hamidi, D. M. Ionel, and A. Nasiri, "Modeling and Management of Batteries and Ultracapacitors for Renewable Energy Support in Electric Power Systems–An Overview," *Electr. Power Components Syst.*, vol. 43, no. 12, pp. 1434–1452, Jul. 2015.

[68] M. B. Camara, H. Gualous, F. Gustin, and A. Berthon, "Design and New Control of DC/DC Converters to Share Energy Between Supercapacitors and Batteries in Hybrid Vehicles," *IEEE Trans. Veh. Technol.*, vol. 57, no. 5, pp. 2721–2735, Sep. 2008.

[69] "RTDS Technologies Inc.: Real Time Digital Power System Simulation." [Online]. Available: https://www.rtds.com/.

Vitae

Name	:Md. Juel Rana
Nationality	:Bangladeshi
Date of Birth	:10/20/1989
Email	:g201403940@kfupm.edu.sa, juelrana.eee@gmail.com
Address	:Dhaka, Bangladesh
Academic Background	:Received B.Sc. in Electrical and Electronic Engineering from Rajshahi University of Engineering & Technology (RUET), Bangladesh in 2011. He has completed M.Sc. in Electrical Engineering from Electrical Engineering Department at King Fahd University of Petroleum and Minerals in January, 2017.
Research Interests	:Power System and Renewable Energy, Microgrid Control, Power Electronic Applications to Power Systems, Artificial Intelligence Applications to Power Systems, Smart Grid and Electric Vehicle.